

Challenge of Understanding Structure-odor Relationships and Development of Olfaction Inspired Odor Sensor Based on Molecular Imprinted Materials

Liang Shang

Graduate School of Information Science and Electrical Engineering,
Kyushu University, Fukuoka, Japan



Introduction

Smell or olfaction

Chemical sense

Odorants

To understand environment

A large gene family (1,000 genes)

1 trillion olfactory stimuli

Purposes



Food foraging



Mating

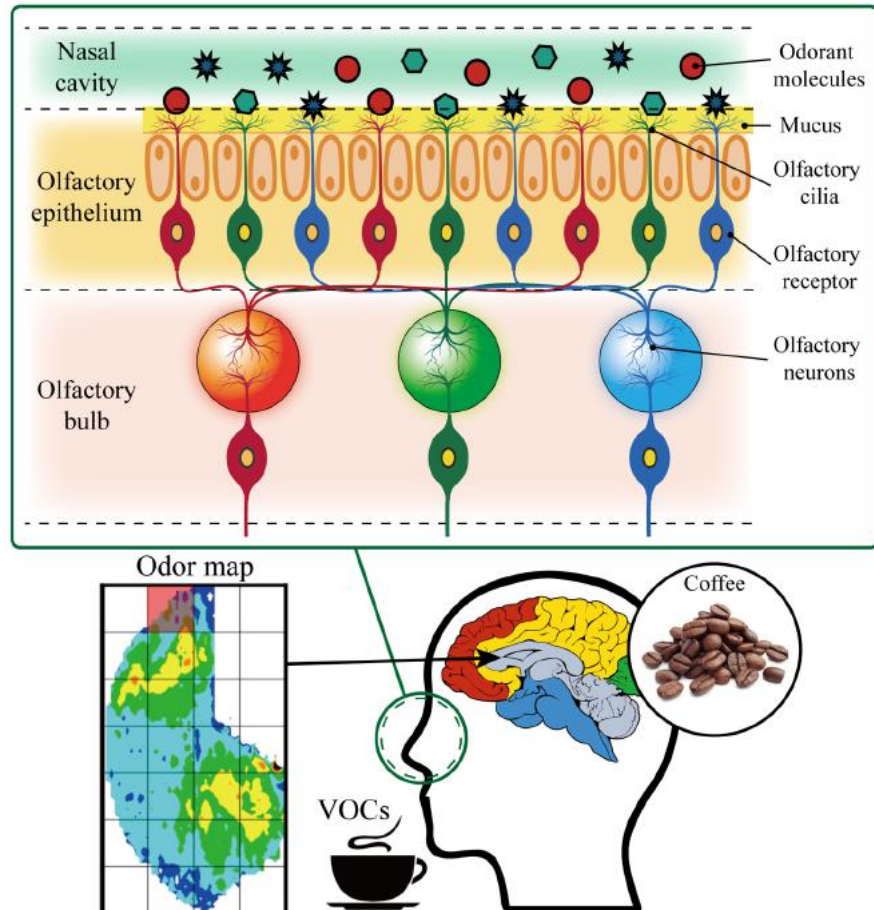


Detection of threats



Trail following

Olfaction and olfaction system



Understand bio-olfaction system

**Molecular features for odorants
(Molecular parameters)**

**Response pattern on olfaction bulb
(Odor map)**

**Odor feelings/descriptions
(Perceptual intelligence)**

Studying the relationship between odor maps and the structural features of odorants can be helpful for understanding the mechanisms underlying olfactory perception.

Olfaction and olfaction system

Odorants with a comparable structure would be smelled similarly

→ **Molecular descriptors**

→ **Mass spectra**

→ **Infrared spectra**

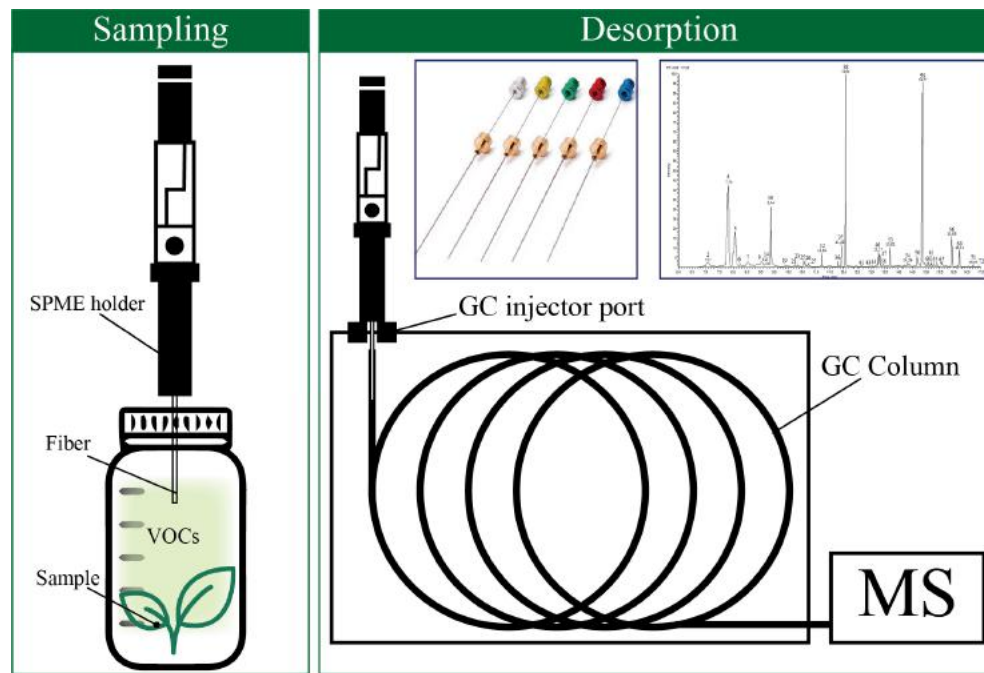


To measure
odorants

The relationship between molecular features and perceptual feelings are still not clear because of its complexity and nonlinearity

Odor detection method

Gas chromatography/mass spectrometer



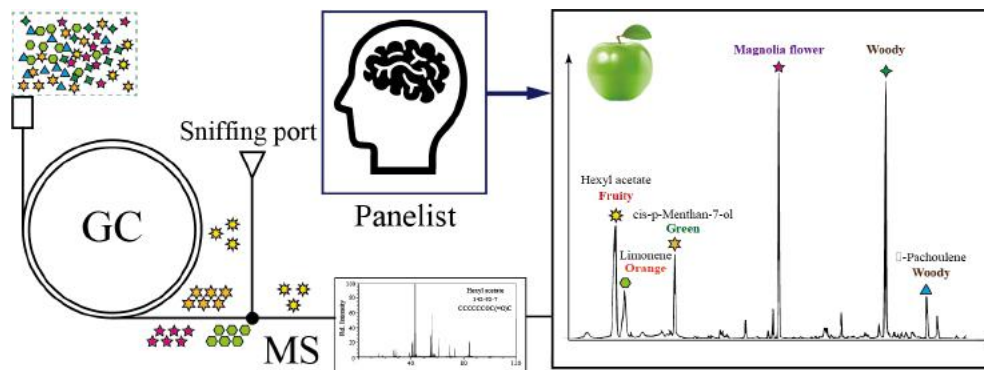
High sensitivity

Mature technology

High-cost

Not portable

Time-consuming

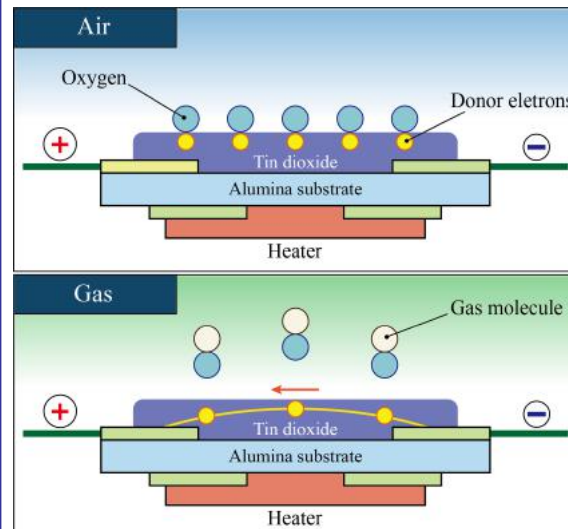


Not suitable for real-time monitoring

Odor detection method

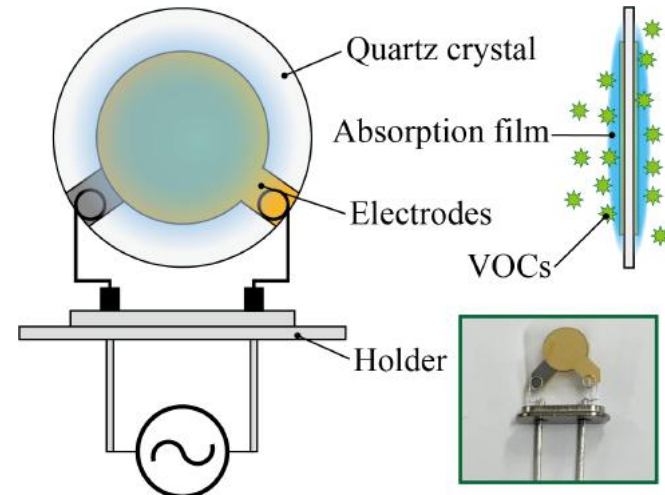
Gas sensors and chemical sensors

Metal Oxide Semiconductor



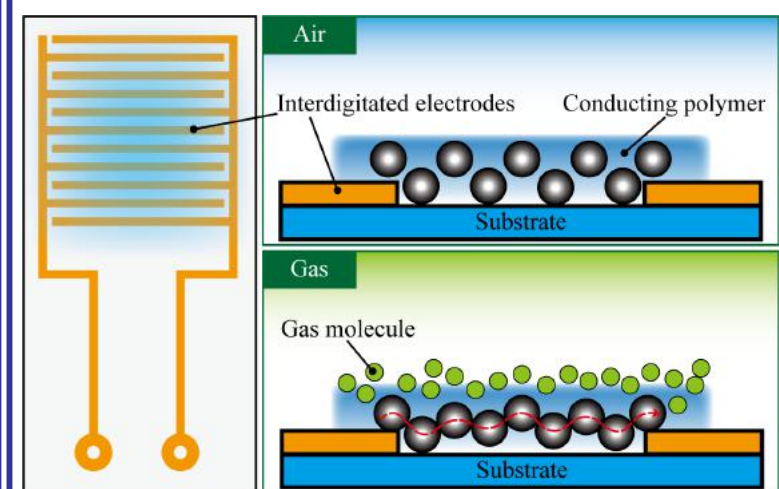
High operating temperatures

Quartz Crystal Microbalance



Easily effected by noise and humidity

Chemiresistors

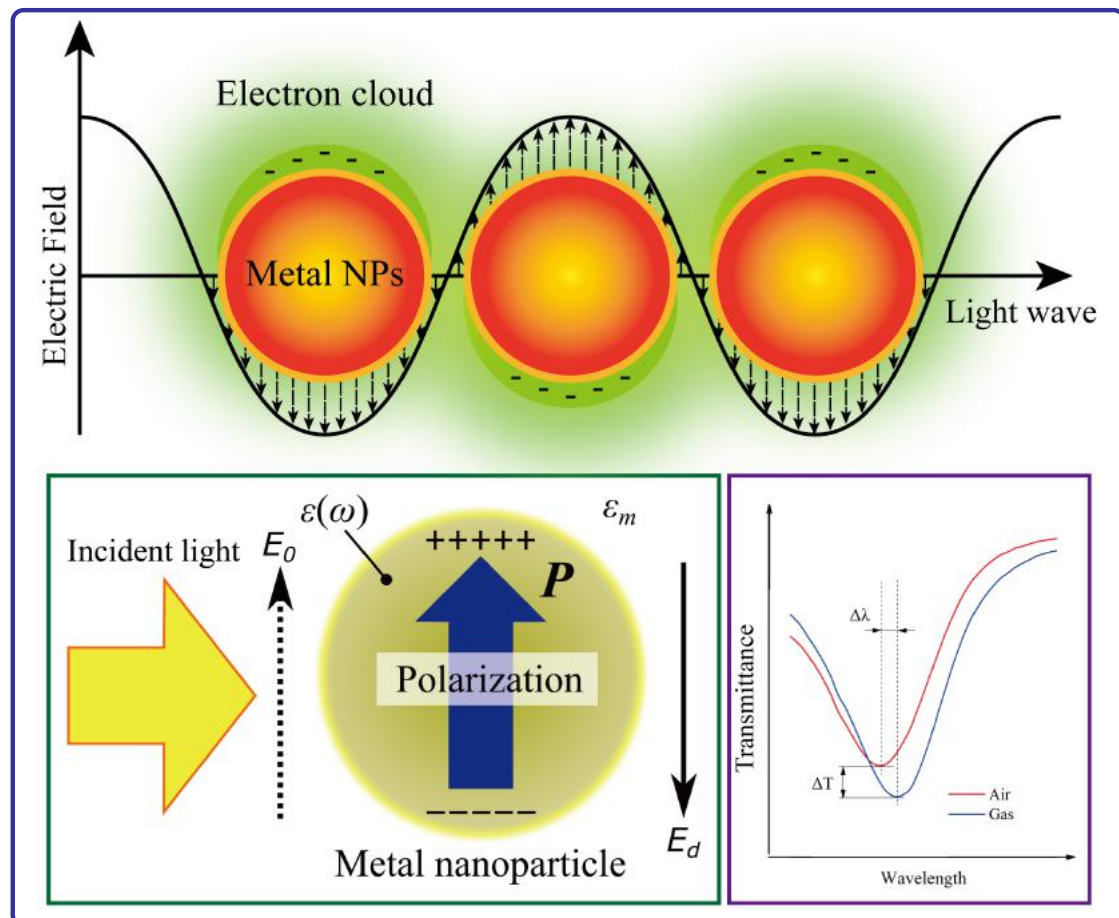


Aging problem

Novel sensors should be developed for VOCs detection with **low cost, high response speed and sensitivity.**

LSPR

Localized surface plasmon resonance (LSPR)



$$P = \frac{3}{4\pi} \frac{\epsilon_m[\epsilon(\omega)-1]}{\epsilon(\omega)+2\epsilon_m} E_0$$

Absorption spectra

Particle size, shape, composition

Surrounding media

Merit & drawback

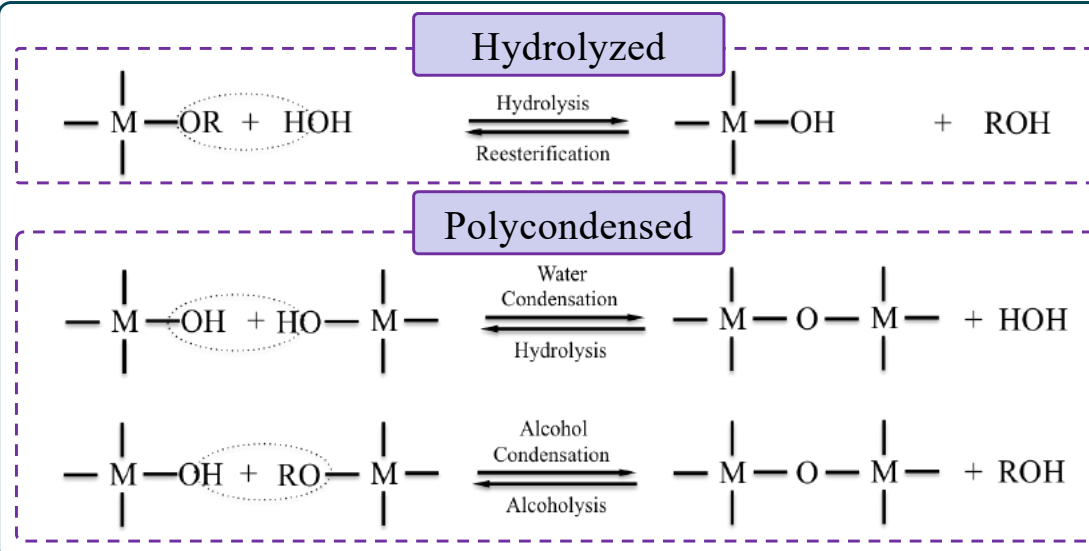
Fast response/recovery speed

Non specificity

MISGs

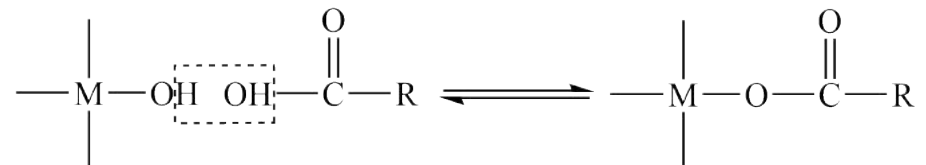
Molecularly Imprinted Sol-gel (MISG)

Reaction principle

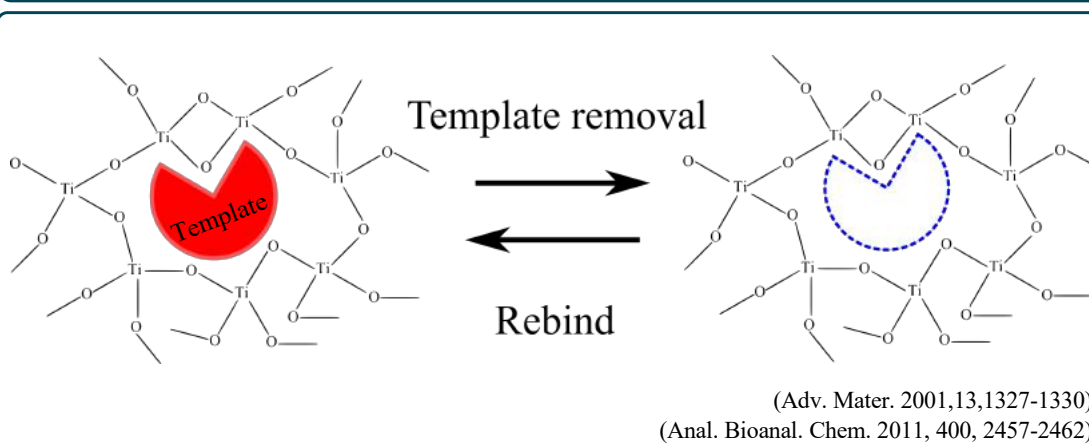
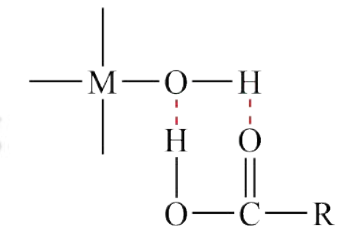


Imprinting method

Covalent bonding



Hydrogen bonding



Compared with other MIP

Stability of
chemical and thermal

Motivation and objectives

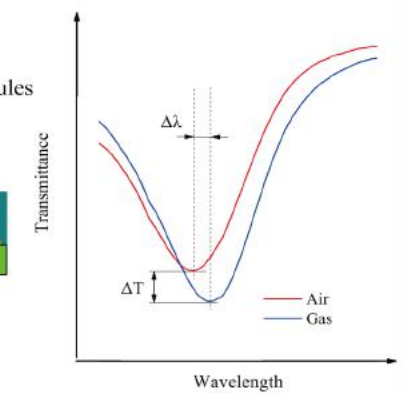
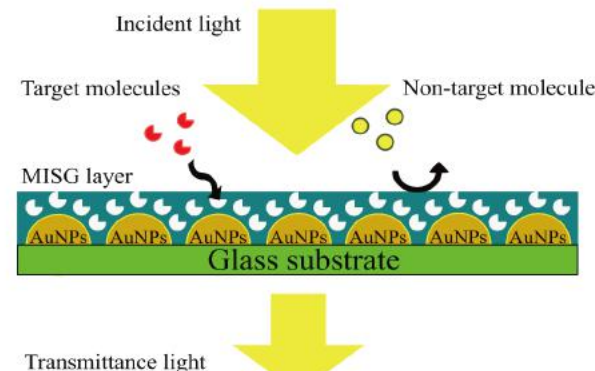


Structure-odor relationship

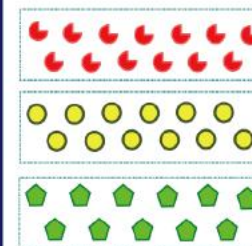
Odor descriptions



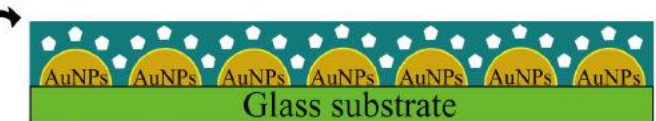
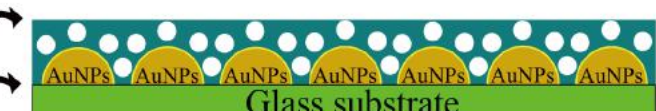
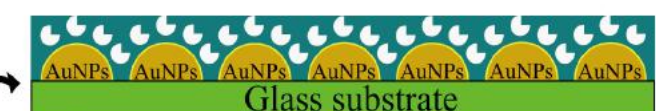
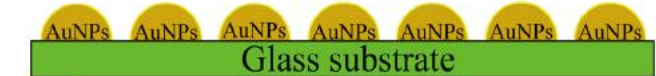
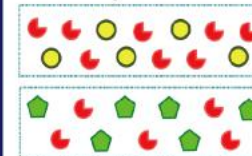
Molecularly imprinted sensor



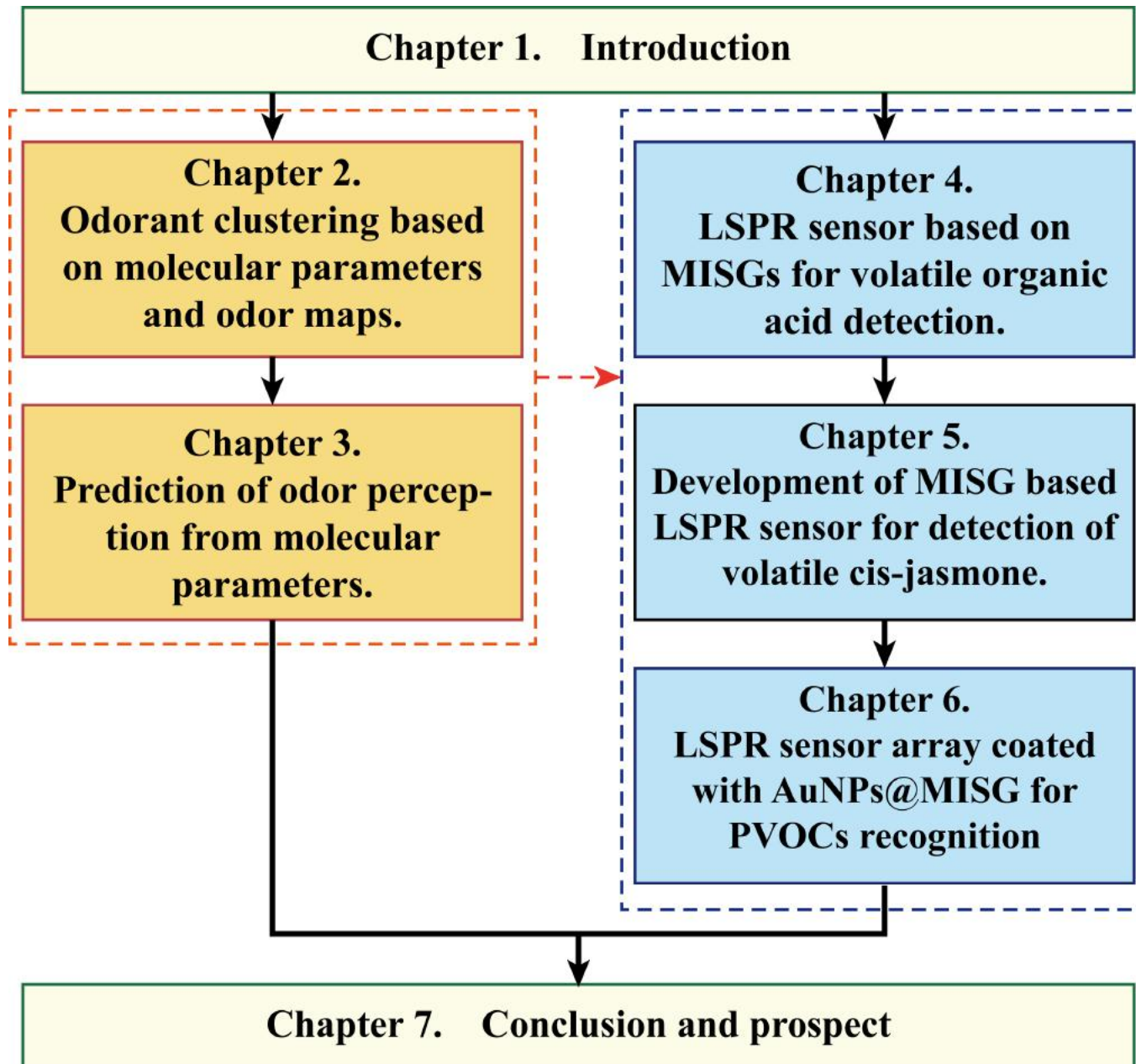
Single gas



Binary mixture



Organization of dissertation



Chapter 2

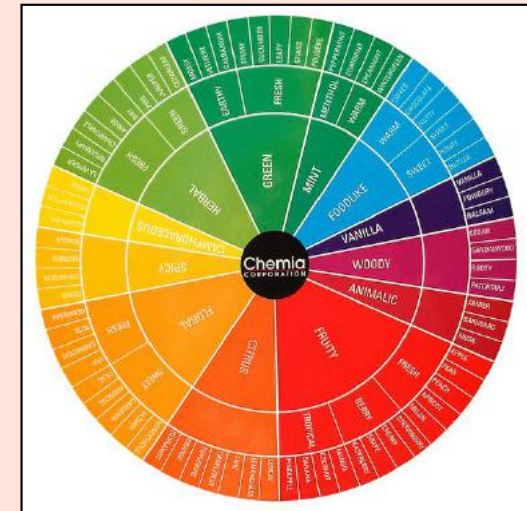
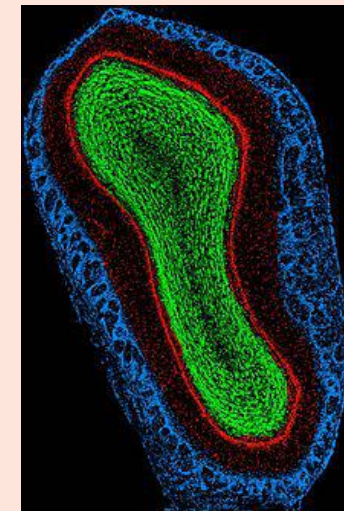
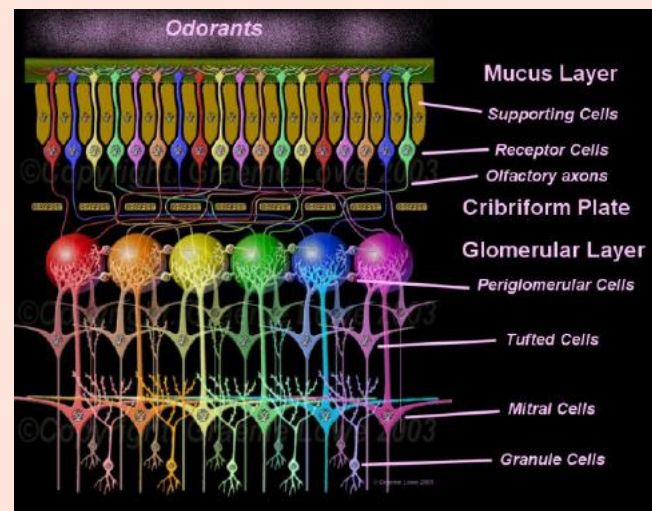
Odorant Clustering Based on Molecular Parameters and Odor Maps



九州大学
KYUSHU UNIVERSITY

Introduction

The mechanism of biological olfaction has become clearer



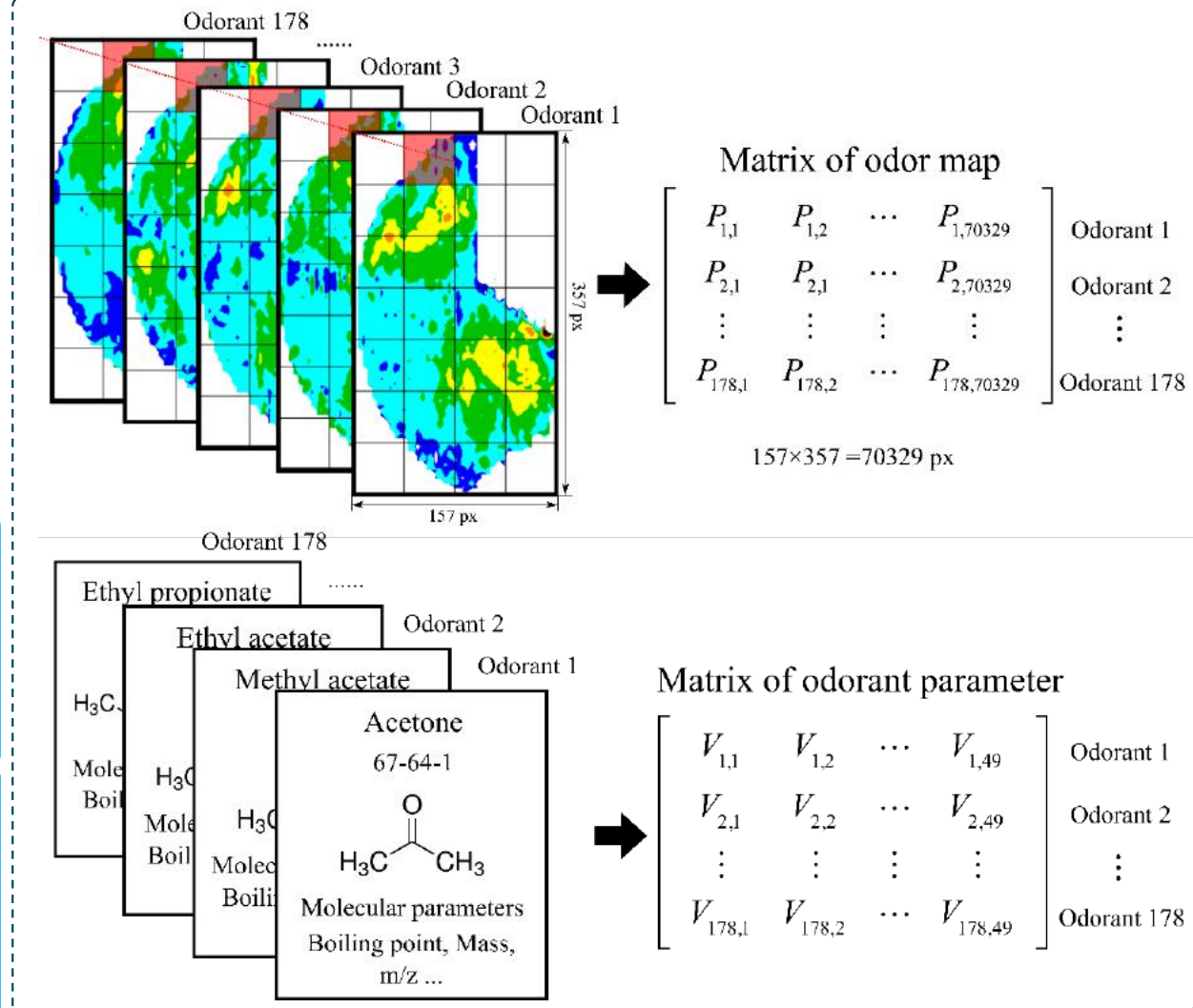
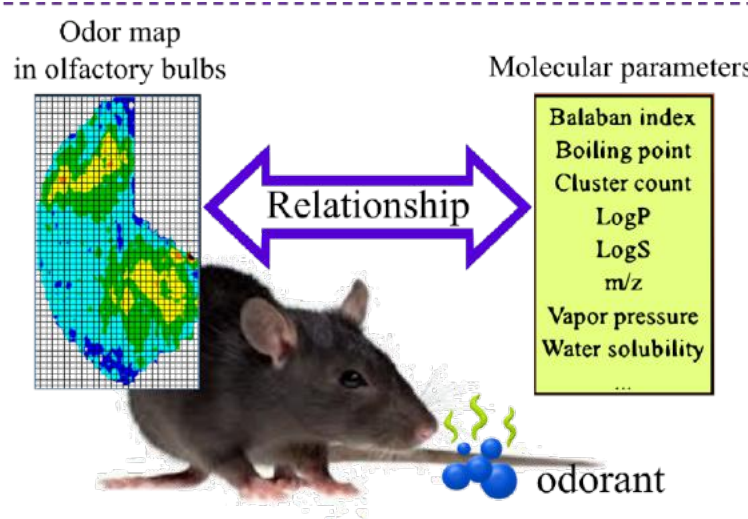
Molecular features
for odorants

Compress

Response pattern
on olfaction bulb

To explore the relationship between odor patterns and their molecular features.

Data description



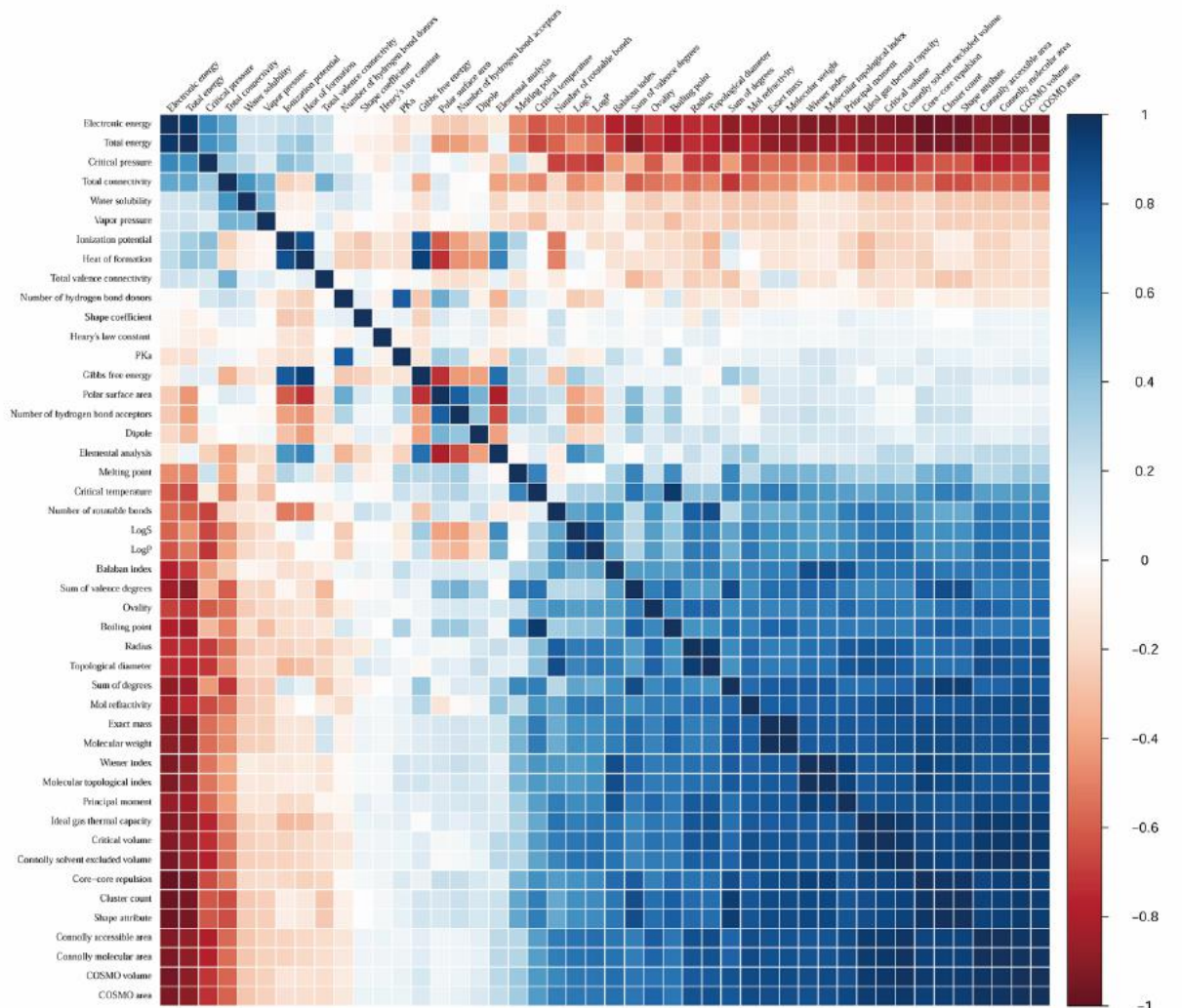
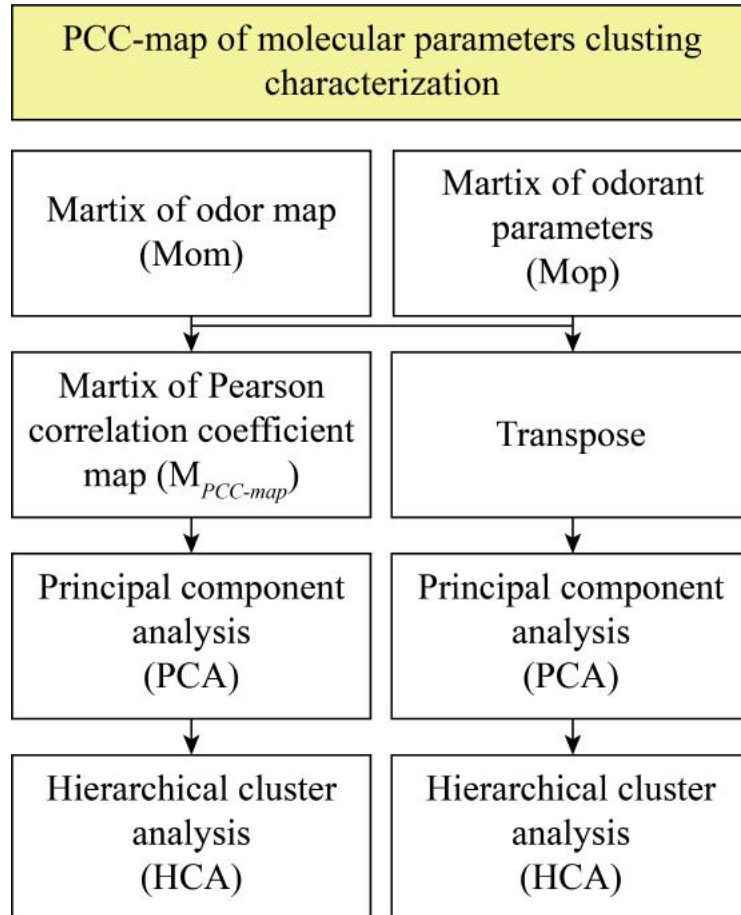
Odor maps:

<http://gara.bio.uci.edu/>

Molecular parameters:
Calculated by ChemBio 3D

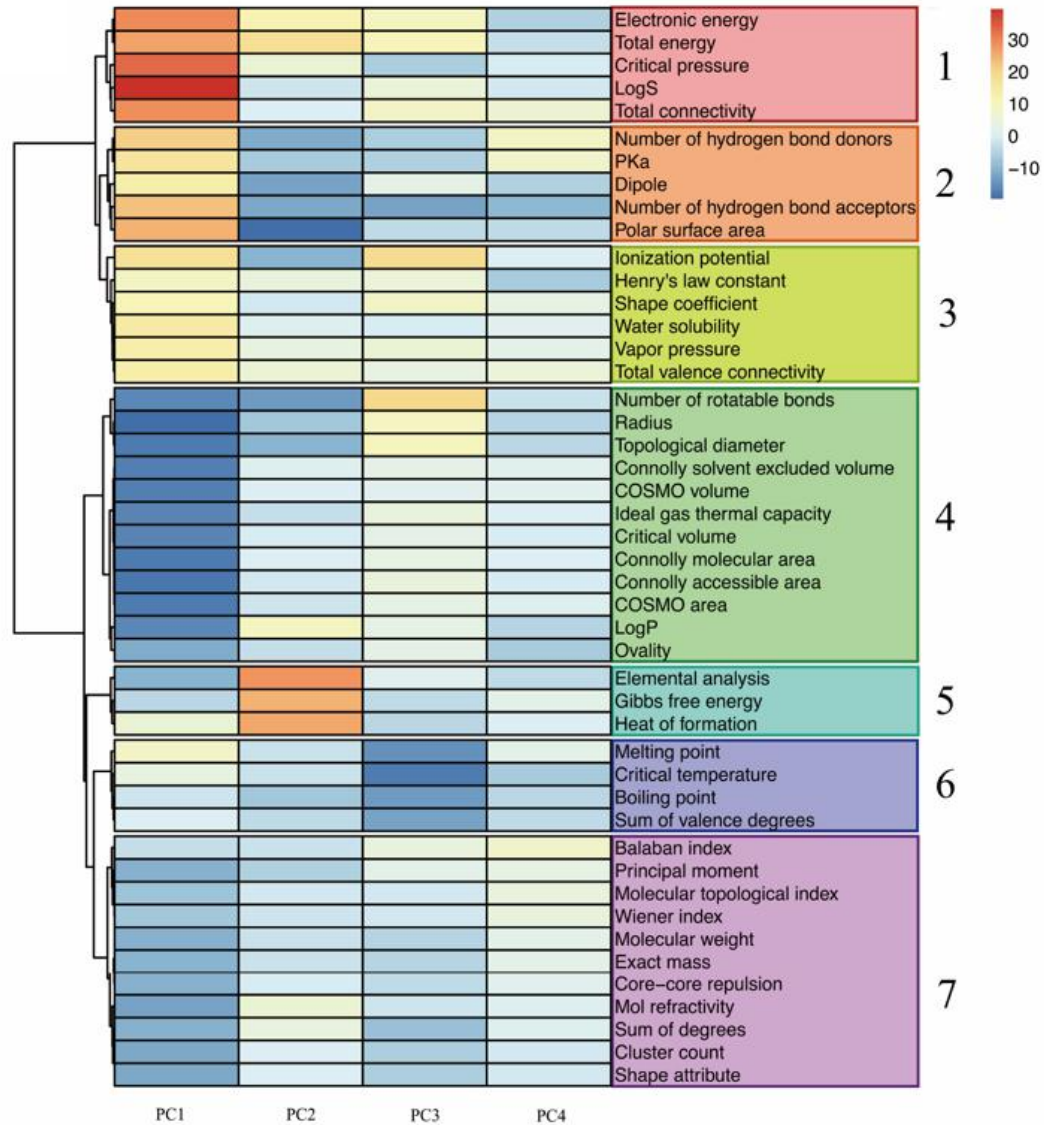
Here, we will talk about these 2 matrixes:
olfaction information and molecular information.

Method

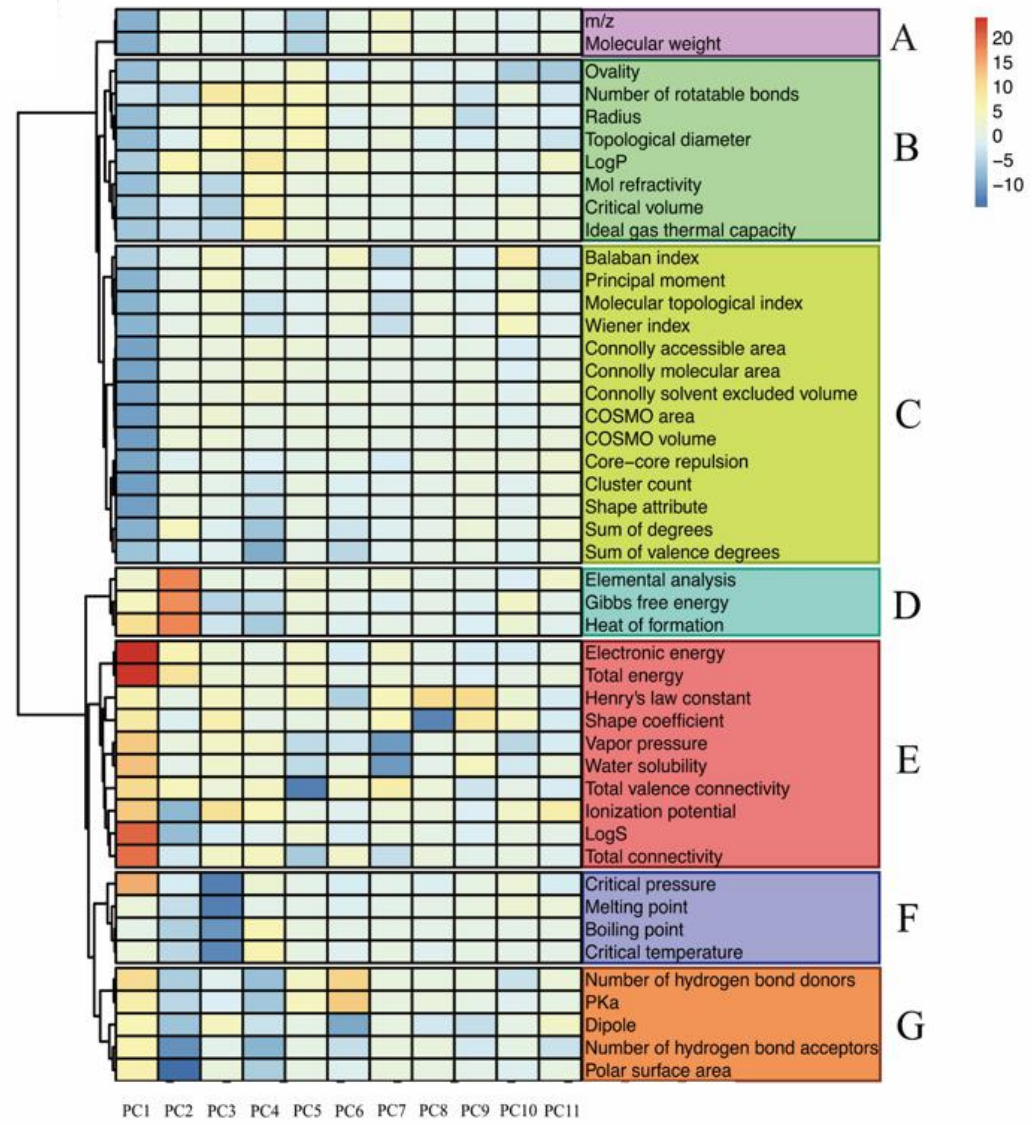


Some parameters are **linearly related** and that some **similar information** is included in the molecular parameter matrix.

PCC-maps

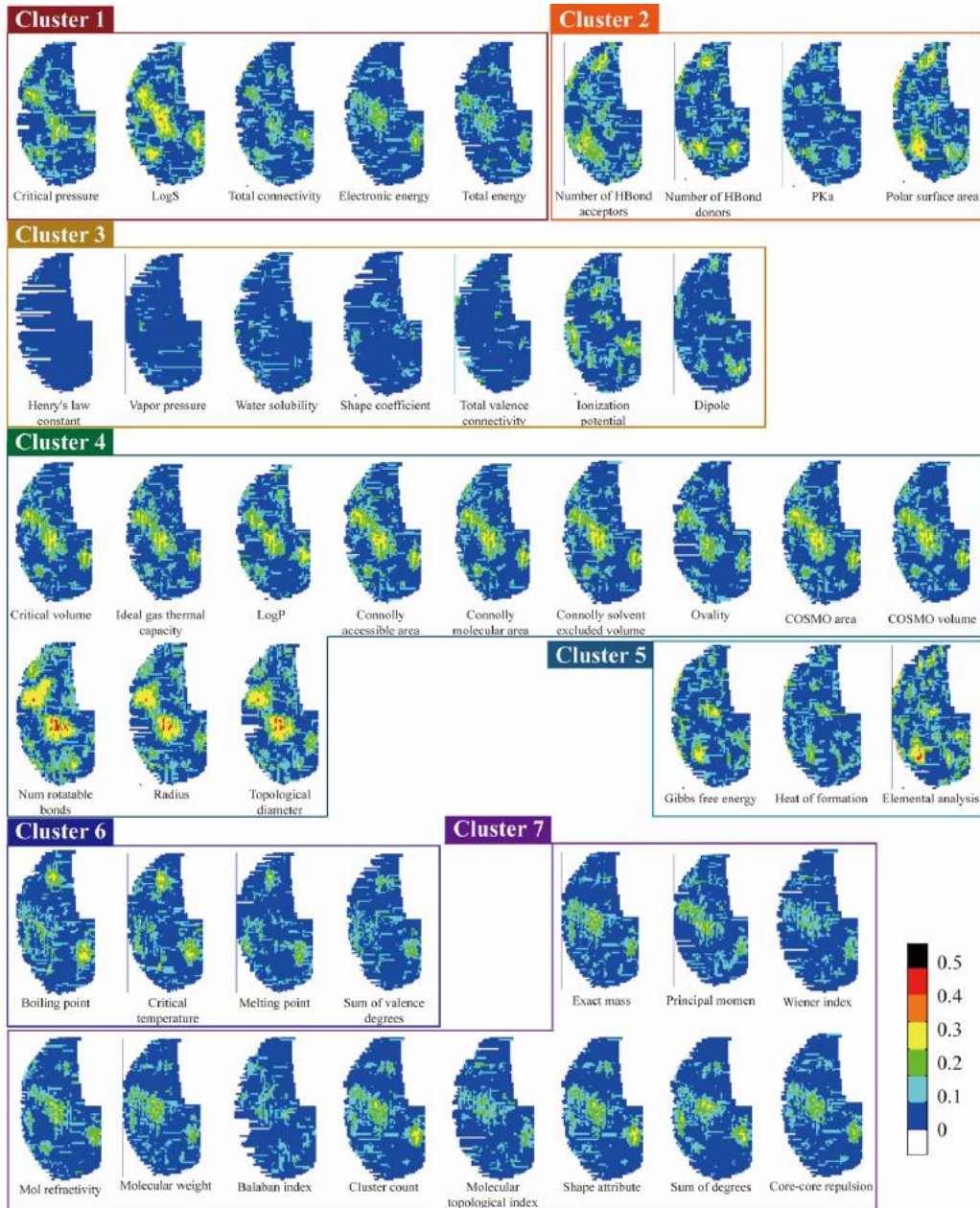


Molecular parameters



- 46 MPs are clustered into 7 clusters.
- Groups visualized by these heat maps shared some similarities to the PCC maps.
(cluster 2 and cluster G, cluster 5 and cluster D, and cluster 6 and cluster F)
- Some parameters are clustered differently.

Results and discussion

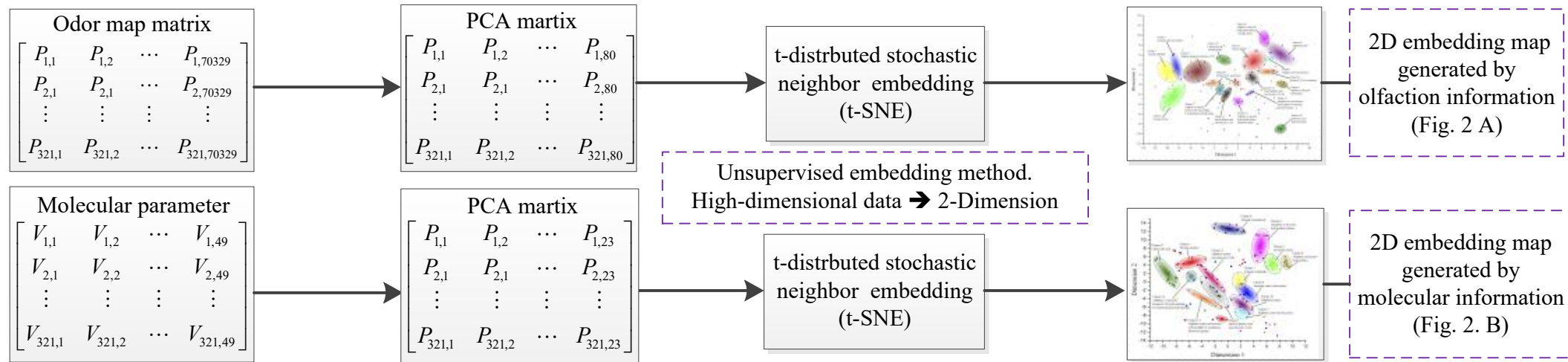


Discussion

- Similar response pattern is shown in each group.
- MPs in the same group could contribute the similar information to OMs.
- Energy information (Cluster 1).
- Polarity information (Cluster 2).
- Low correlation coefficients indicated that the relationships are non-linear.

Method

To establish 2D artificial cluster maps



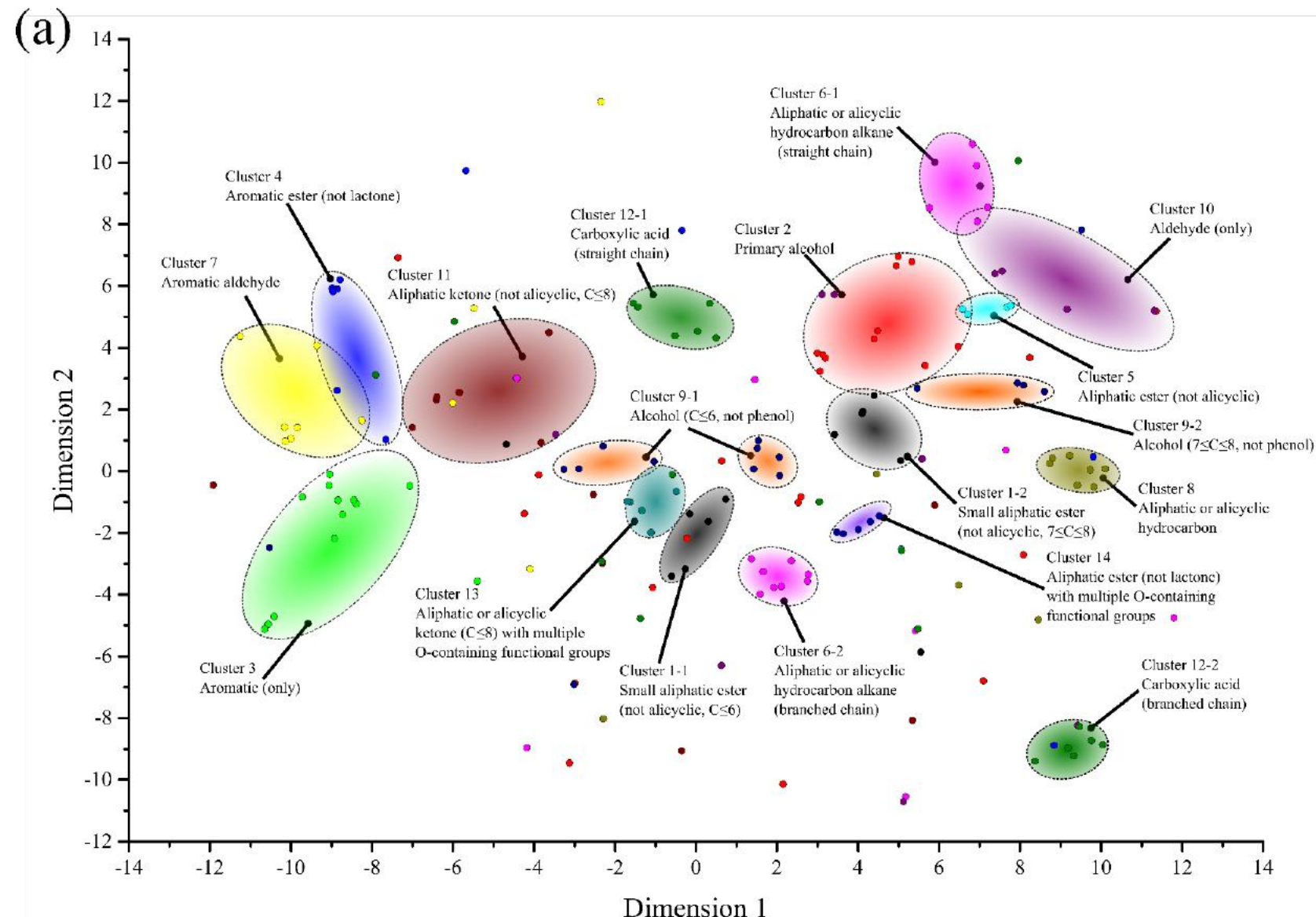
t-distributed stochastic neighbor embedding (t-SNE)

- Nonlinear, unsupervised (Self supervised)
- Information compression method.

Based t-SNE, high dimensional data would be expressed in a 2D space.

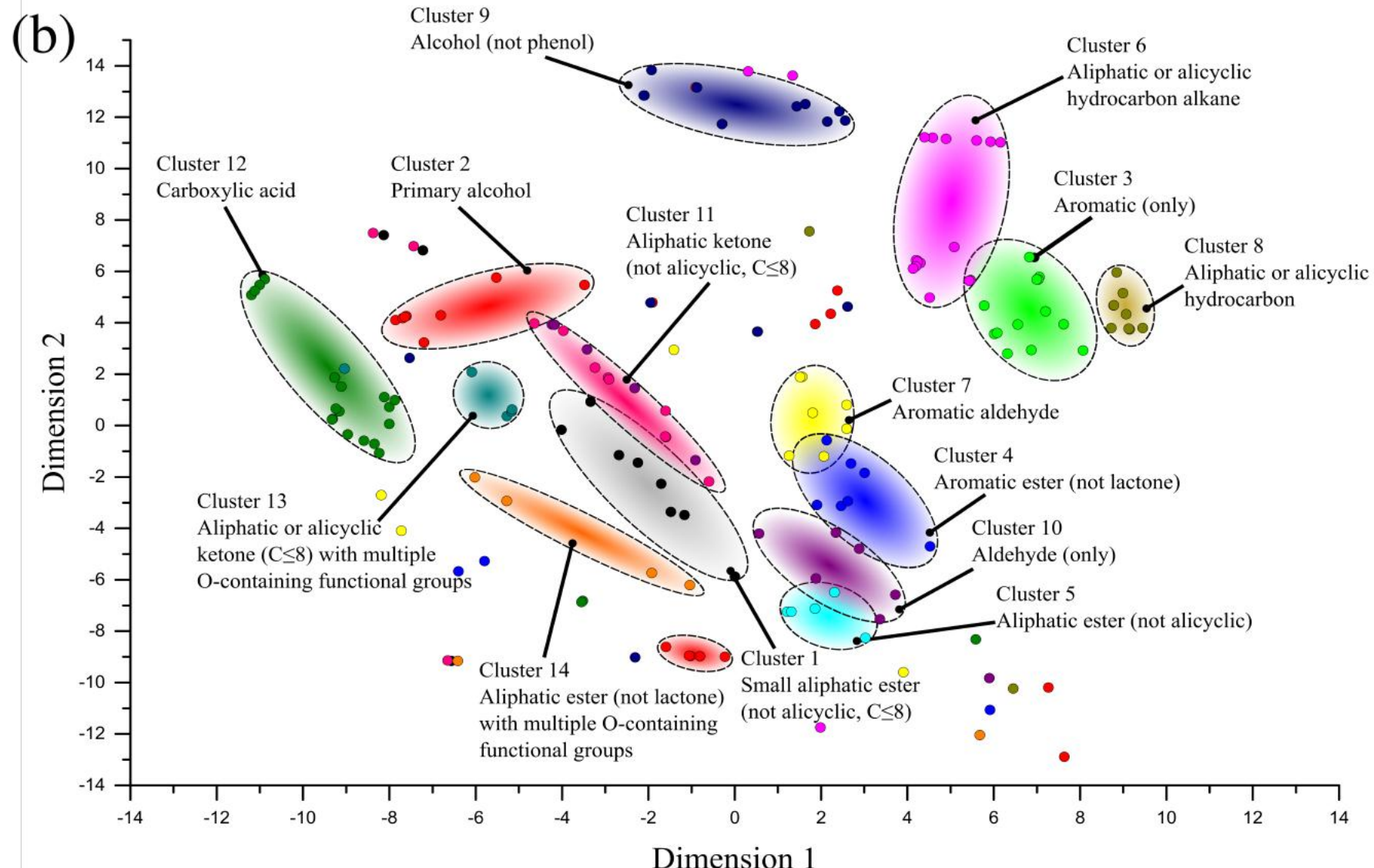
Results and discussion

2D embedding map based on olfaction information



Results and discussion

2D embedding map based on molecular information



Method

To establish functional group discriminating model

Data set

Odor map matrix

Molecular information matrix

Feature extraction method

Principal component analysis (PCA)

T-distributed stochastic neighbor embedding (t-SNE)

Principal component analysis (PCA)

T-distributed stochastic neighbor embedding (t-SNE)

Modeling method (Supervised)

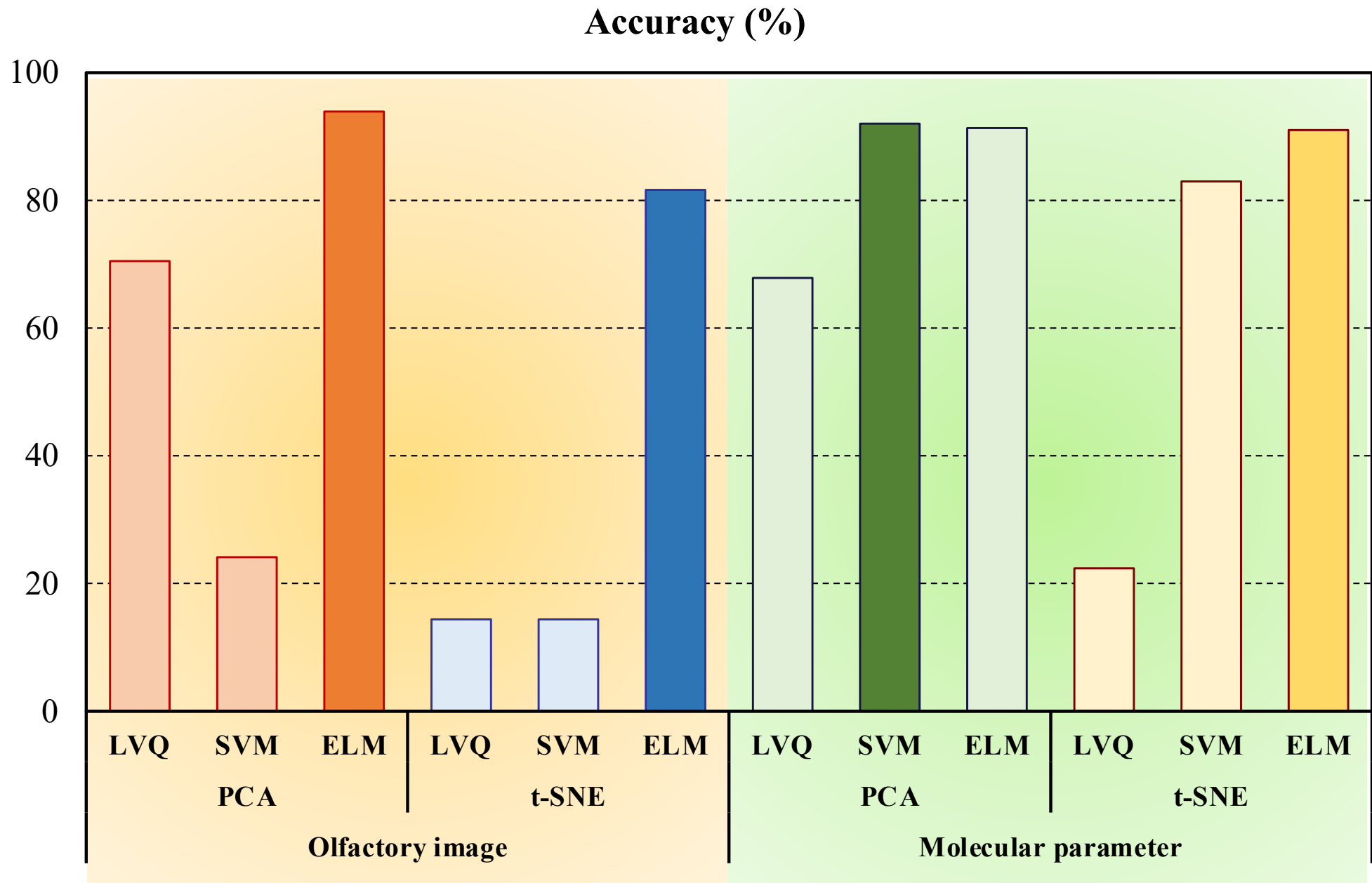
Learning vector quantization (LVQ)

Support vector machine (SVM)

Extreme learning machine (ELM)

Comparation

Results and discussion



Conclusion

- 2D artificial map was established by odor maps or MPs based on t-SNE method.
- It indicated that 46 MPs were mostly to instead of olfaction ideally.
- Functional groups identification models were calibrated.
- Although models calibrated by MPs were weaker than odor maps, a comparative model would be established based on more enough molecular features.

Chapter 3

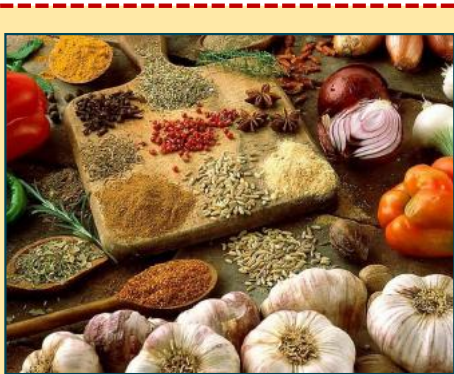
Prediction of Odor Perception from Molecular Parameters



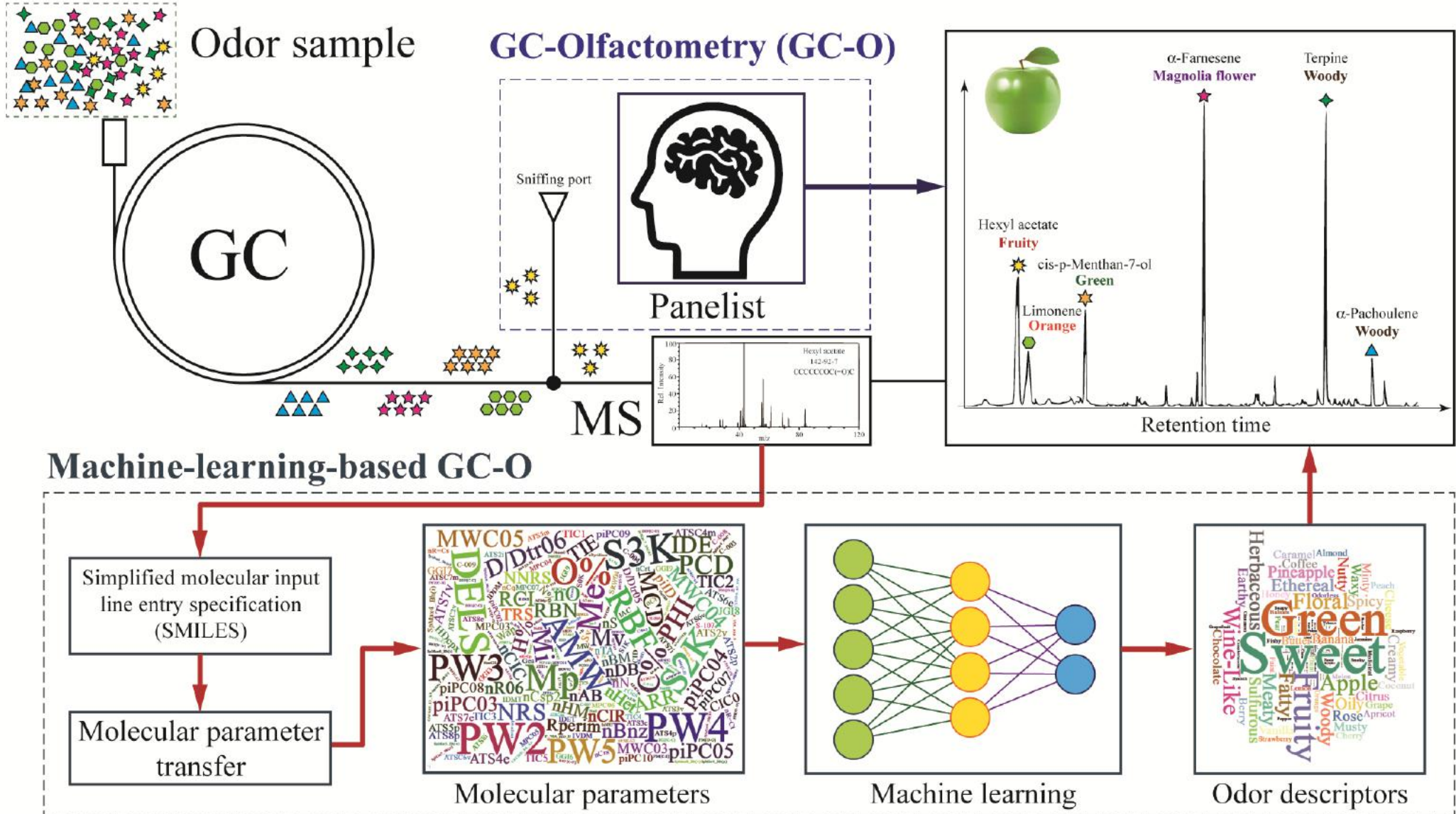
九州大学
KYUSHU UNIVERSITY

Introduction

We want to know the sensory description in an aroma.

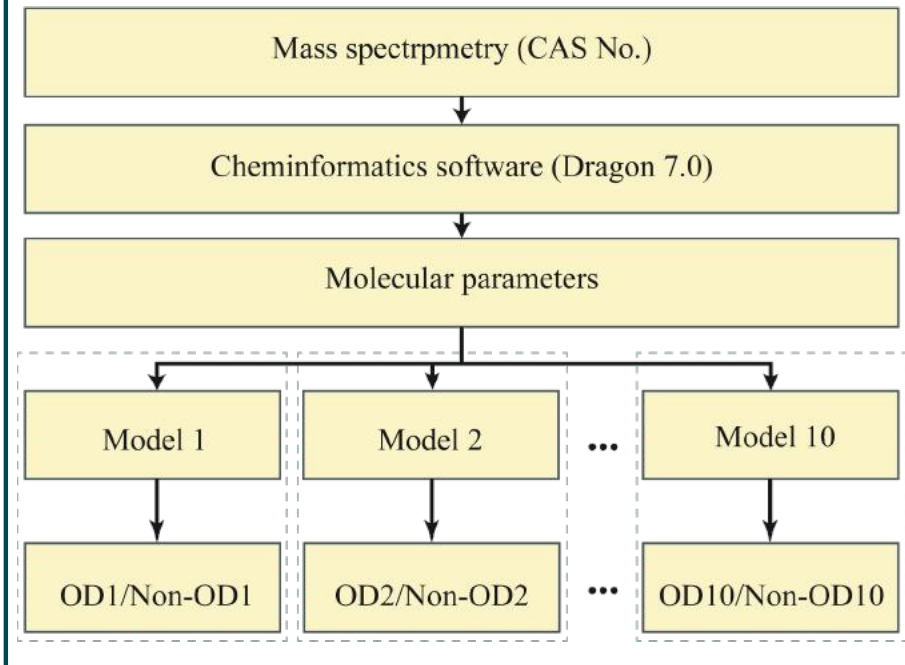


Machine-learning GC-O



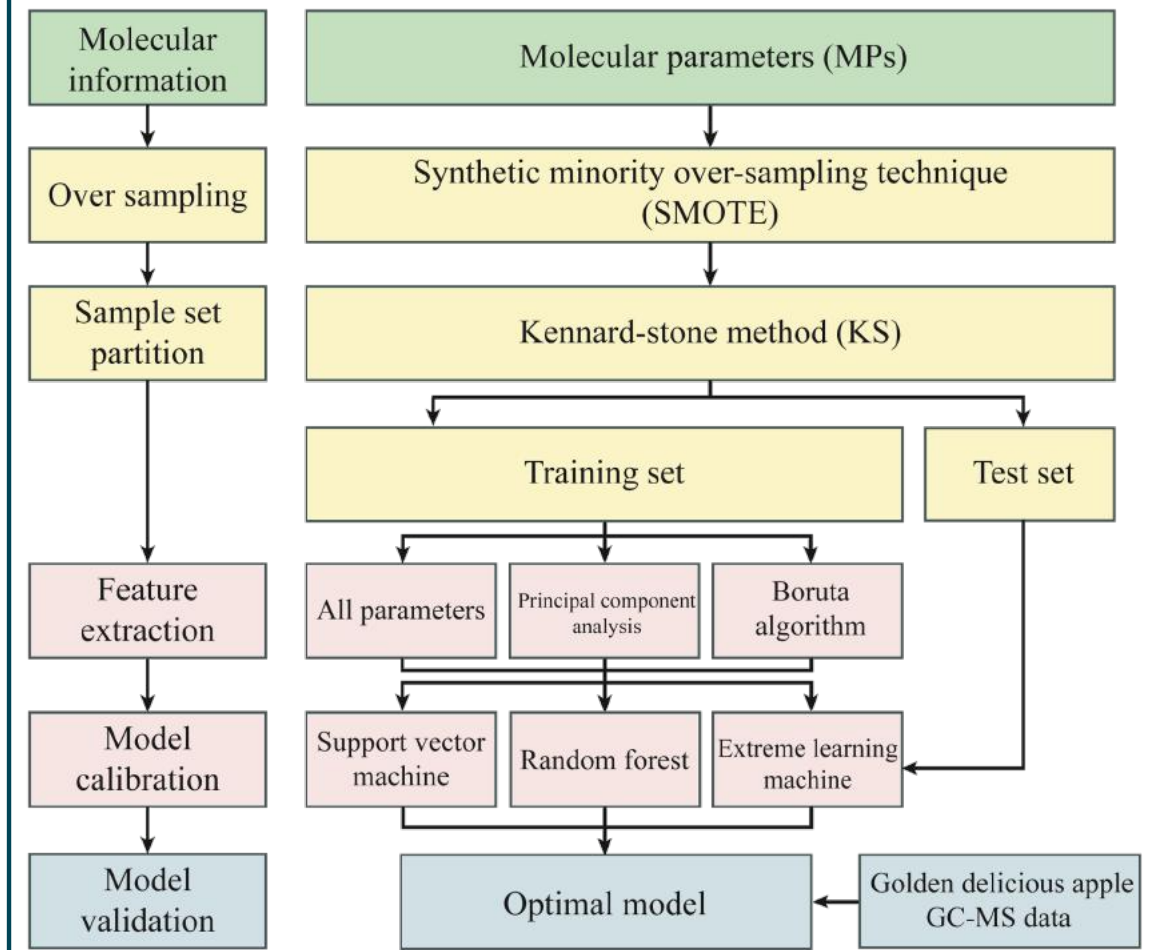
Concept model

Concept diagram



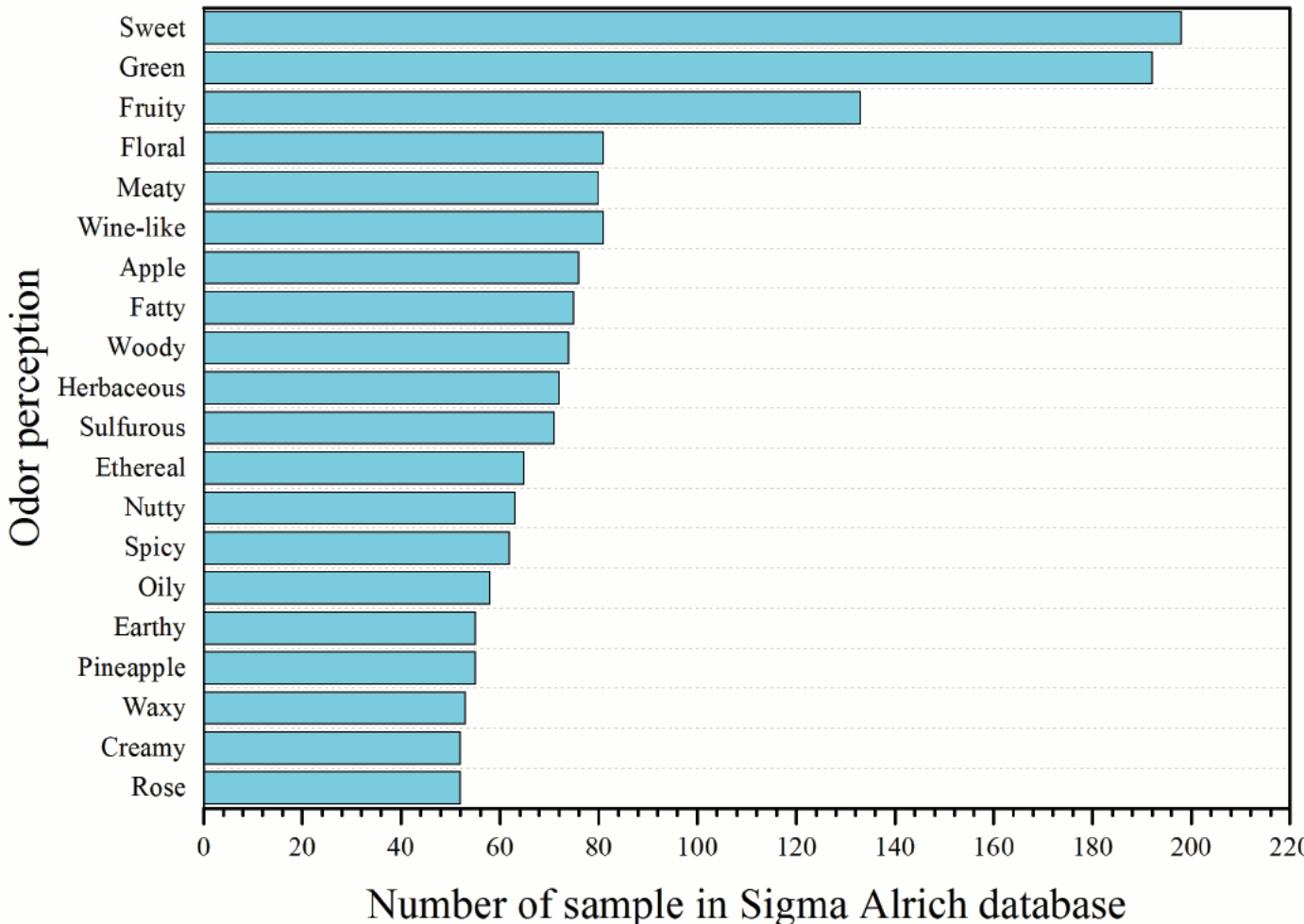
1006 types of molecular parameters.
 1037 odorants in Sigma-Aldrich
 (2016). By Dragon 7.0.

Data processing diagram



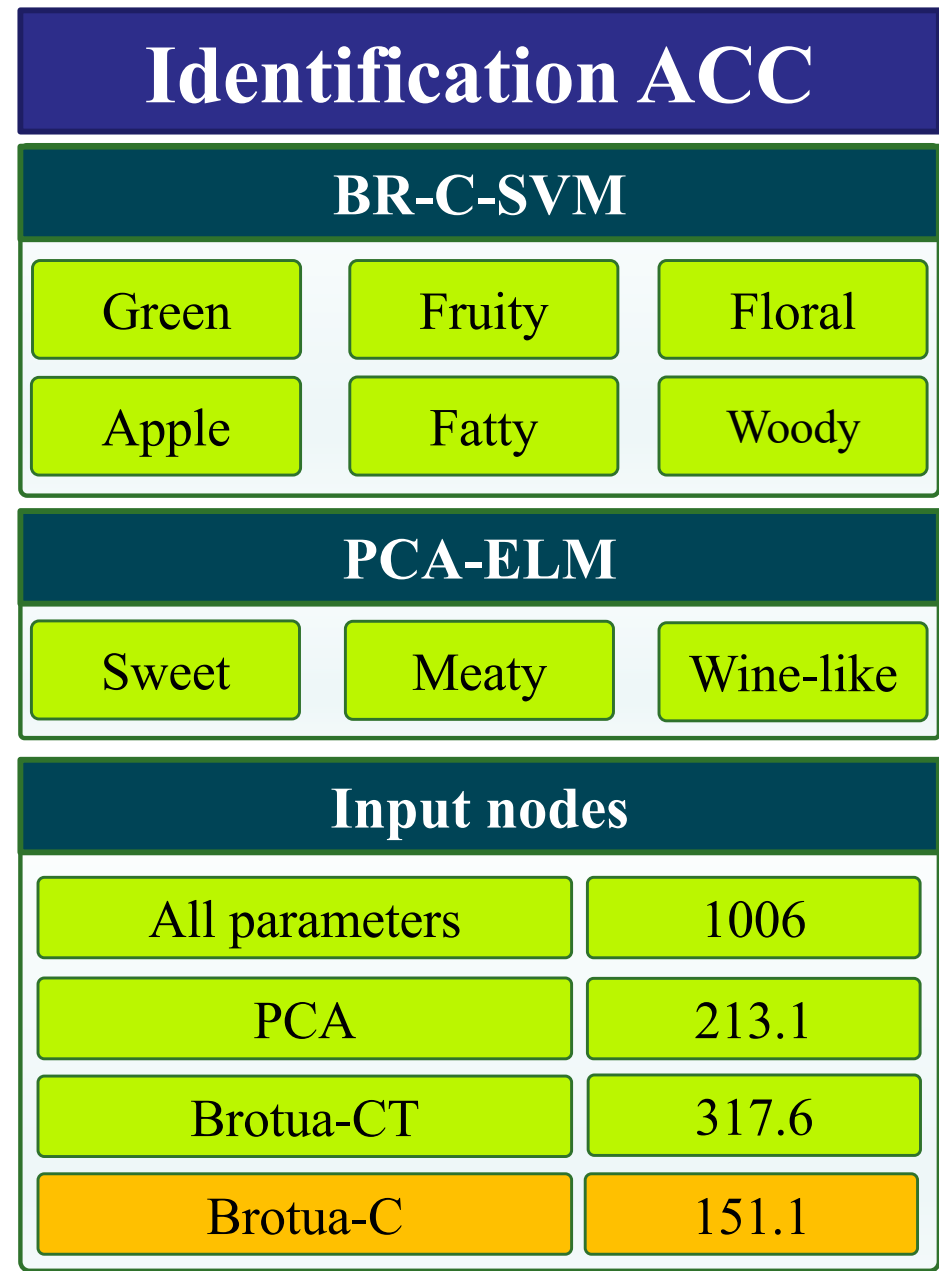
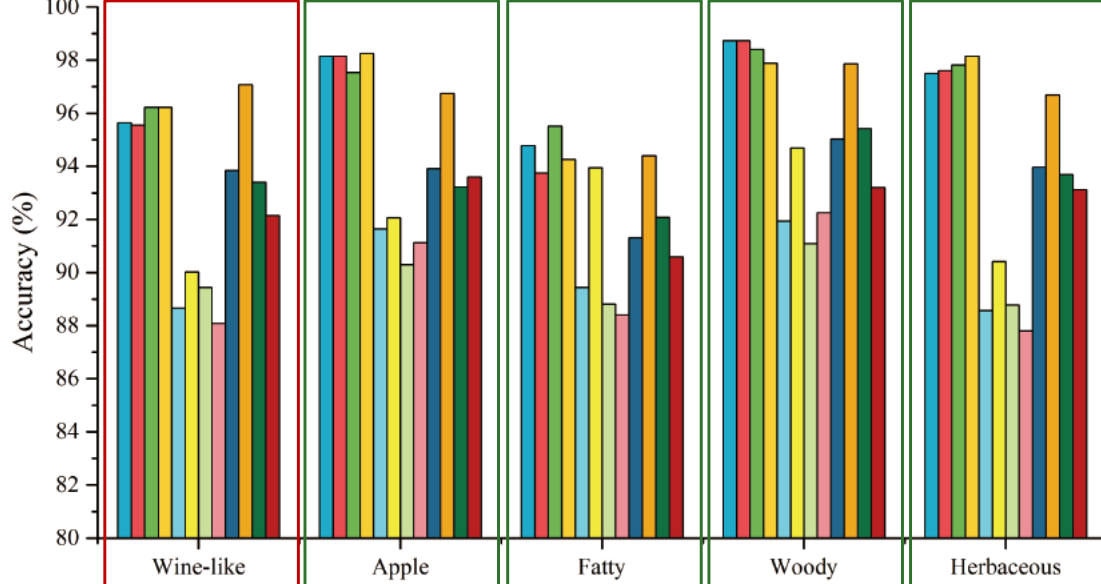
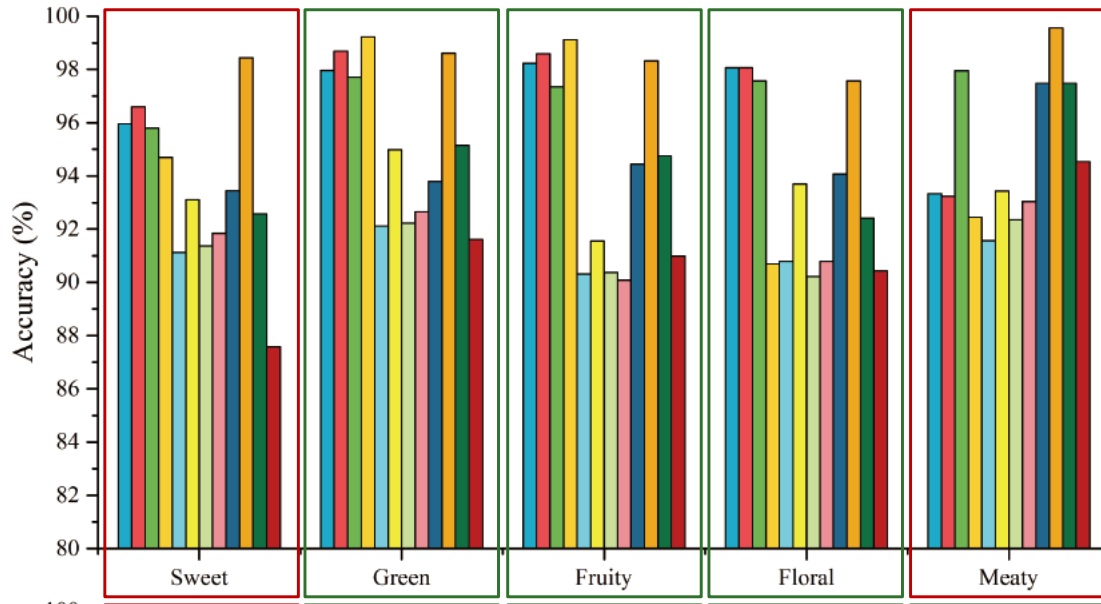
Apple's GC-MS was used to validate the models

Results and discussion



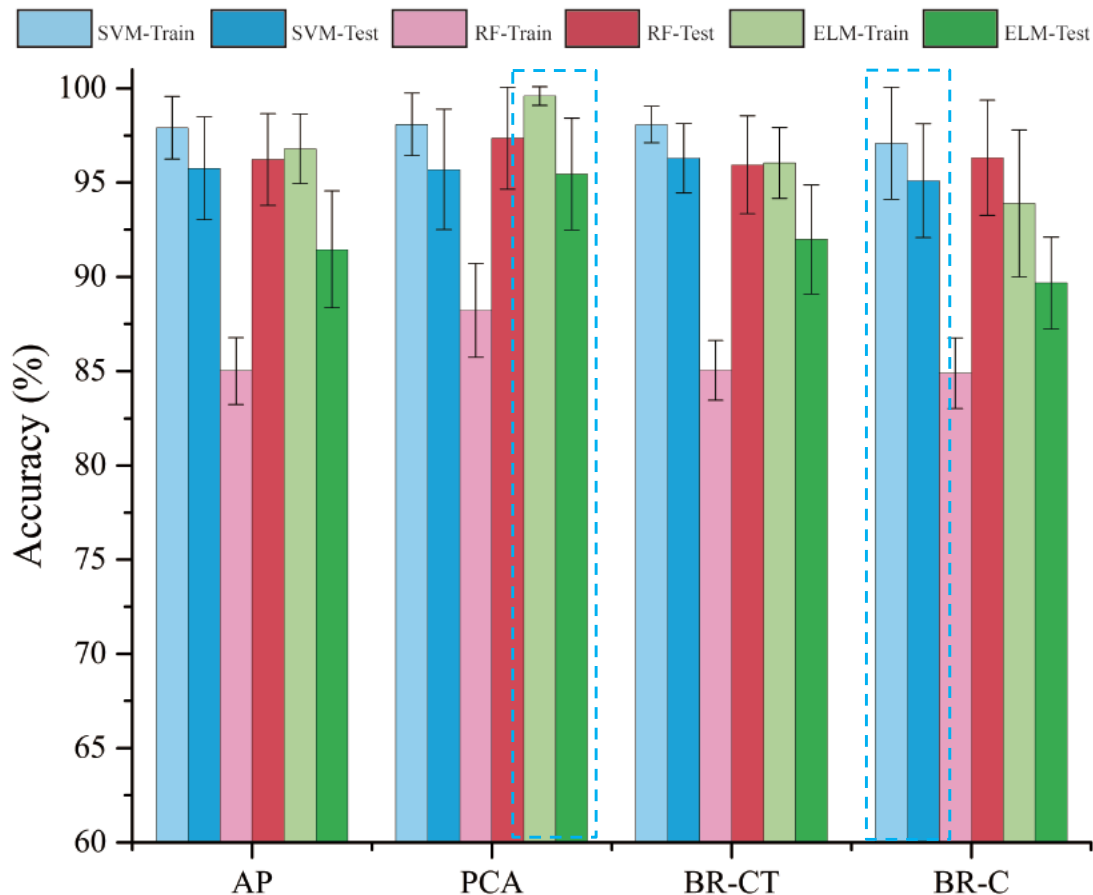
- Twenty most frequent ODs in Sigma–Aldrich database.
- The first 10 odor descriptors were considered in this study.

Results and discussion



Results and discussion

Comparation the performances of models



Optimal model

- PCA did better jobs than Boruta in RF and ELM models.
- The accuracy of PCA-ELM model is the highest ($97.53 \pm 1.35\%$).
- Based on BR-C method, 15.01 % (151.1) parameters can be extracted to instead all MDs (1006).
- It is suggested that BR-C-SVM, was the optimal model ($97.19 \pm 0.93\%$).

Results and discussion

Model Validation by Golden Delicious Apple Sample

No.	Volatile Organic Compound	Odor descriptor from database*	Predicted odor descriptor	No.	Volatile Organic Compound	Odor descriptor from database*	Predicted odor descriptor
1	2-propanol	Alcohol; butter	-	16	Butyl propanoate	Banana; ethereal	Apple
2	1-propanol	Alcohol; <u>apple</u> ; musty; earthy; peanut; pear; sweet	<u>Apple</u>	17	Amyl acetate	<u>Fruity</u> ; banana; earthy; ethereal	<u>Fruity</u> , apple
3	1-butanal	Apple; chocolate; creamy; <u>green</u> ; meaty; ethereal; pear; pungent	<u>Green</u> , fruity	18	(E)-2-hepten-1-al	<u>Fruity</u> ; rose; <u>fatty</u> ; almond-like	Green, <u>fruity</u> , apple, <u>fatty</u>
4	Ethyl acetate	Solvent-like; fruity; anise; ethereal; pineapple	-	19	6-methyl-5-hexen-2-one	Fruity; citrus-like; strawberry	-
5	2-methyl-1-propanol	<u>Fruity</u> ; whiskey; <u>wine-like</u> ; solvent-like	<u>Fruity</u> , <u>wine-like</u>	20	Butyl butanoate	<u>Apple</u> ; banana; berry; peach; pear	<u>Apple</u>
6	1-butanol	Banana; vanilla; fruity	-	21	Hexyl acetate	<u>Apple</u> ; banana; cherry	<u>Apple</u> , fatty
7	Propyl acetate	<u>Fruity</u> , floral	<u>Fruity</u>	22	2-ethyl-1-hexanol	Oily; rose; sweet	Woody, herbaceous
8	2-methyl-1-butanol	Onion; malty	-	23	Butyl 2-methyl butanoate	<u>Apple</u> ; chocolate	<u>Apple</u>
9	1-pentanol	Sweet; vanilla; balsamic	-	24	1-octanol	<u>Fatty</u> ; citrus; waxy; <u>woody</u>	<u>Fatty</u> ; <u>woody</u>
10	Isobutyl acetate	<u>Apple</u> ; banana; ethereal; pear; pineapple	<u>Apple</u>	25	1-nonanal	Apple; coconut; <u>fatty</u> ; fishy	<u>Fatty</u>
11	1-hexanal	<u>Fatty</u> ; <u>green</u>	<u>Green</u> , <u>fatty</u>	26	Hexyl butanoate	Green; <u>fruity</u> ; <u>apple</u> ; waxy	<u>Fruity</u> , wine-like, <u>apple</u> , fatty
12	Butyl acetate	Banana; <u>green</u> ; sweet	<u>Green</u>	27	P-allylanisole	Alcohol; <u>green</u> ; minty; <u>sweet</u> ; vanilla	Sweet; <u>green</u> ; floral
13	(E)-2-hexen-1-al	Almond; <u>apple</u> ; <u>green</u> ; vegetable	<u>Green</u> , <u>apple</u> , fatty	28	Hexyl 2-methyl butanoate	<u>Green</u> ; <u>fruity</u> ; <u>apple</u> ; grapefruit-like	<u>Green</u> ; <u>fruity</u> ; <u>apple</u> ; herbaceous
14	1-hexanol	<u>Green</u> ; <u>herbaceous</u> ; <u>woody</u>	<u>Green</u> , fatty, <u>woody</u> , <u>herbaceous</u>	29	Hexyl hexanoate	<u>Green</u> ; vegetable; <u>fruity</u> ; <u>apple</u> ; cucumber-like	<u>Green</u> ; <u>fruity</u> ; fatty
15	2-methyl-1-butyl acetate	Banana; peanut; fruity, apple-like	-	30	(E, E)- α -farnesene	Green; herbaceous	-

Results and discussion

- It indicated that 70% (21/30) of compounds were predicted accurately.
- The other seven compounds were shown to be unpredictable, which can be explained by the **insufficient number of OD models** calibrated in presented research.
- Some ODs, such as peanut and balsamic, were not considered in the present study because of their smaller samples.
- Additionally, the predicted accuracy would be increased by consideration of **more odorant samples** and establishment of **enough OD models**.

Chapter 4

LSPR Sensor Based on MISGs for Volatile Organic Acid Detection

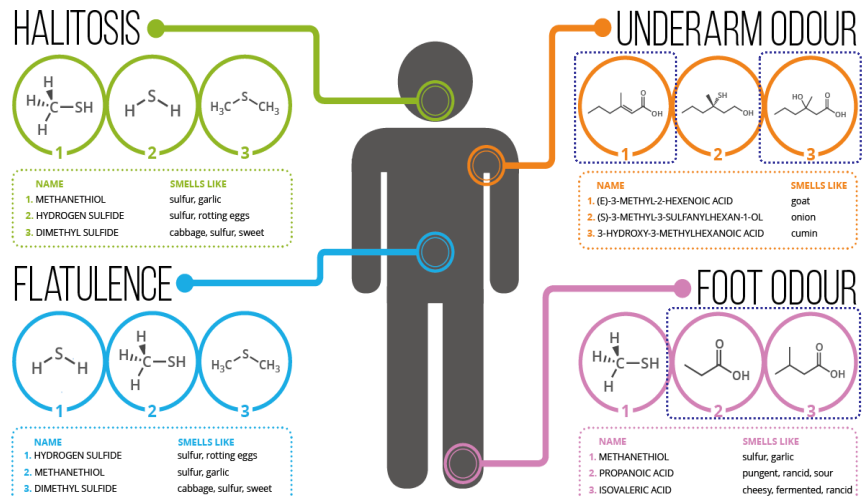


Introduction

Body odor

THE CHEMISTRY OF BODY ODOURS

Body odour is the result of bacterial activity producing odorous compounds. Here, we look at some of the main compounds in particular odours.



Application



Medical diagnosis



Physiological condition

Volatile organic compounds (VOCs)

Fatty acids

Alcohols

Aldehydes

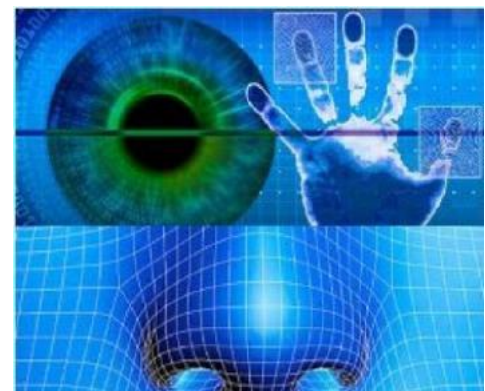
Esters

Ketones

Amines



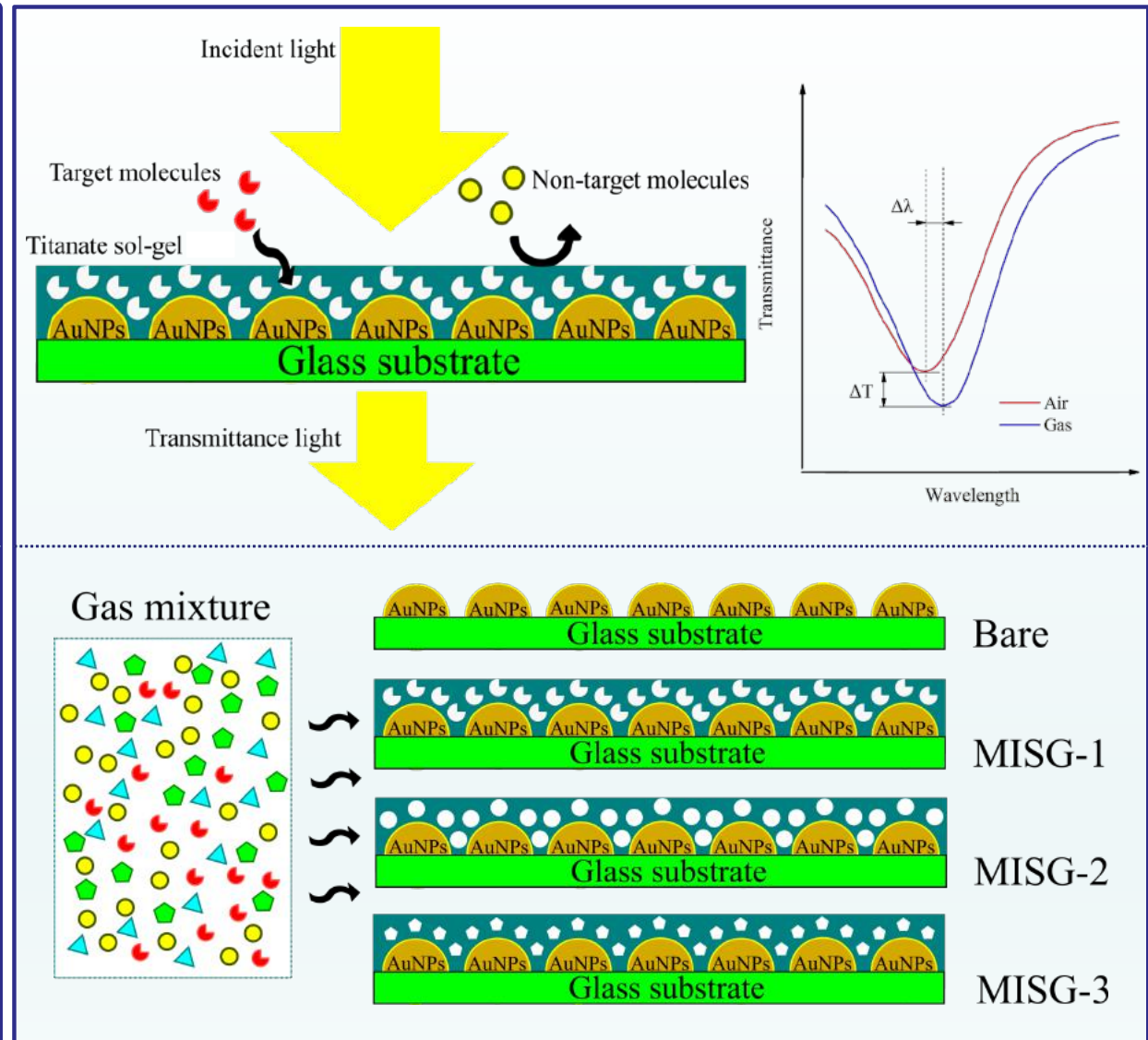
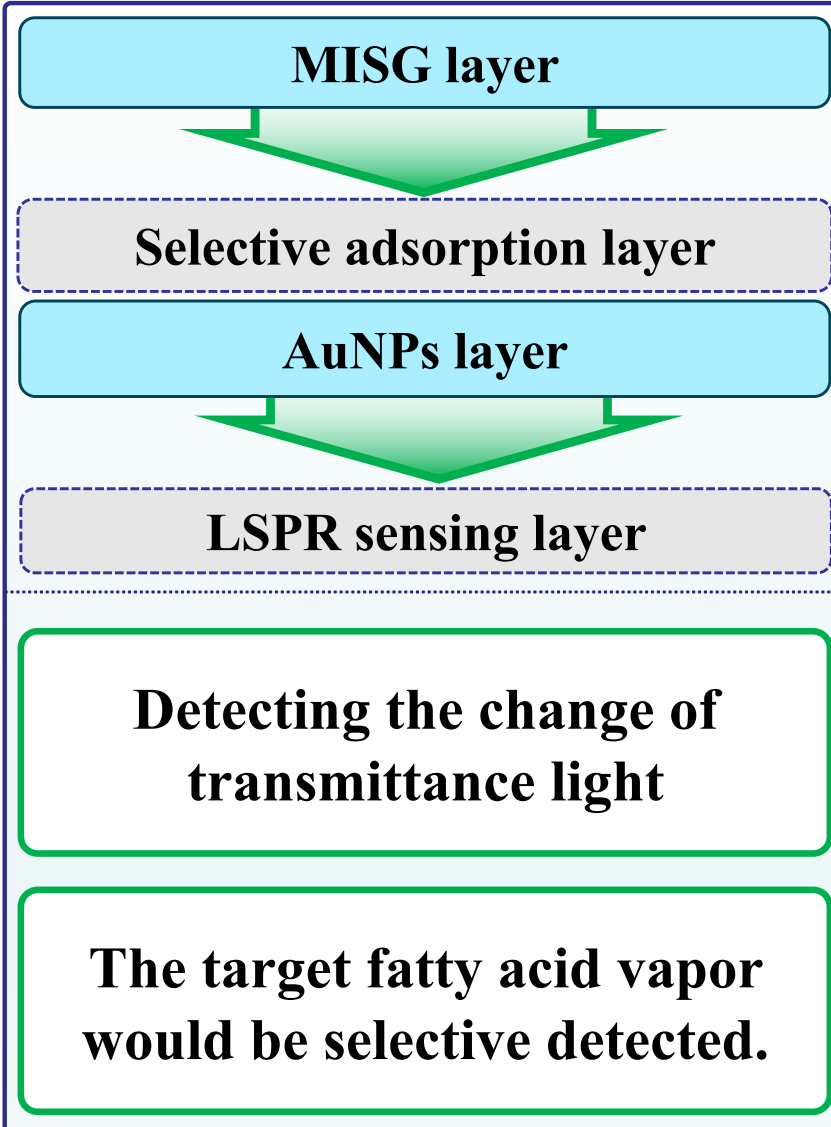
Forensic



Body odor fingerprint

Concept

MISG-LSPR sensor array



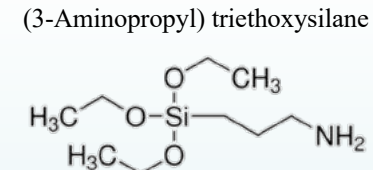
Experiment

MISG material

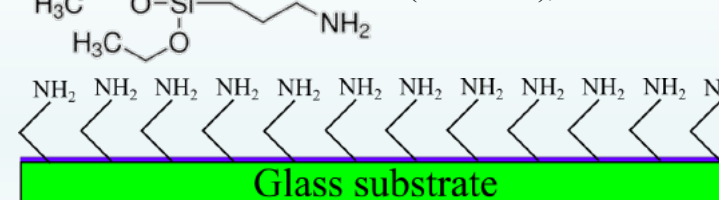
Iso-propanol	2 mL
Ti(OBu) ₄	136 μ L
APTES	24 μ L
Template	50 μ L
TiCl ₄	25 μ L

MISG-AuNPs film fabrication

Step 1 APTES modification

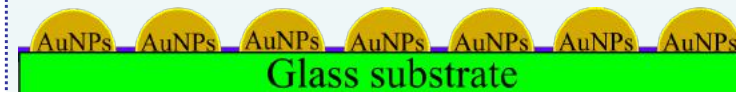


APTES ethanol solution
(v:v = 1:10), 8 h



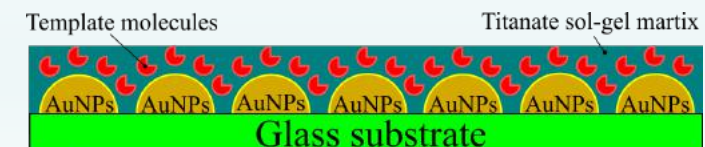
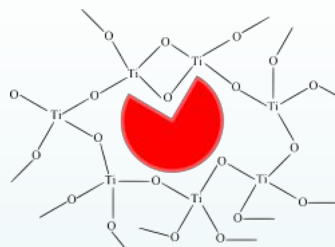
Step 2 Sputtered AuNPs and anneal

Sputtering AuNPs thickness: 3nm
Anneal: 200 °C, 5h, air



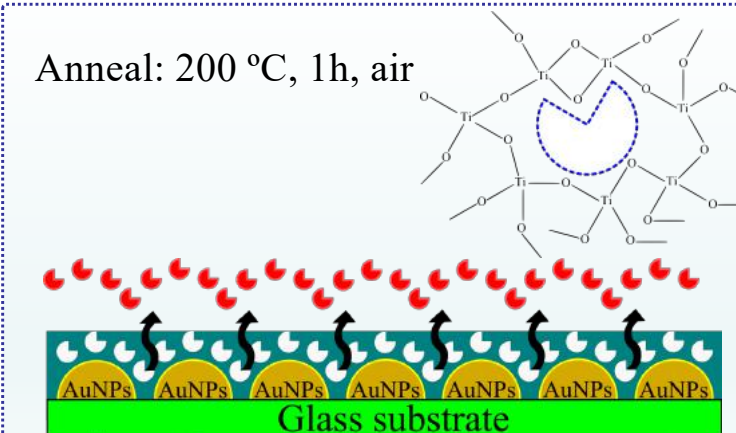
Step 3 MISG reaction solution spin coating

MISG solution: 20 μ L
Spin coating speed:
1000/3000/5000 rpm



Step 4 Annealed for removing templates

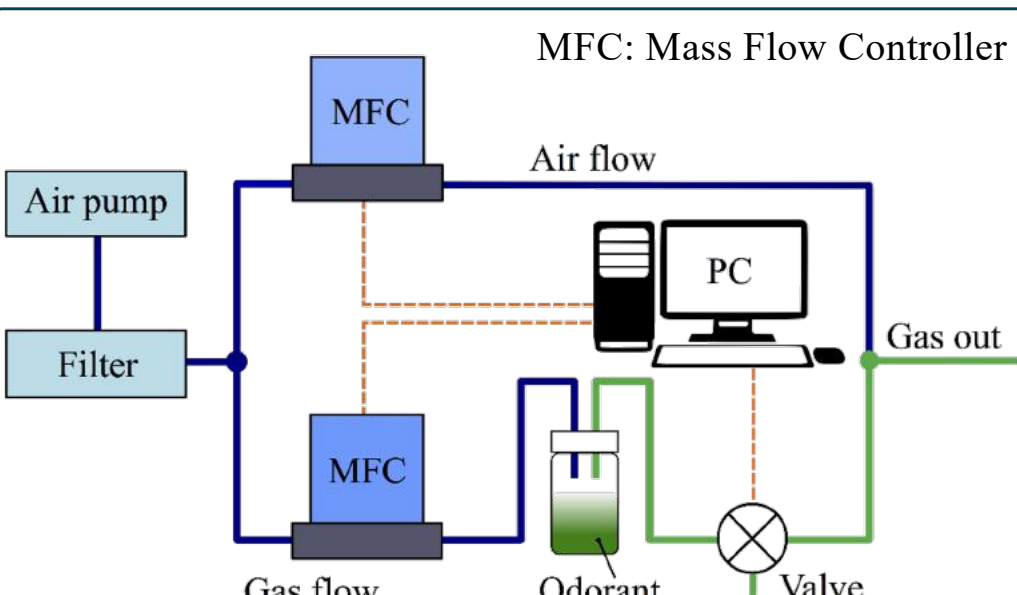
Anneal: 200 °C, 1h, air



70 °C water bath, 1h

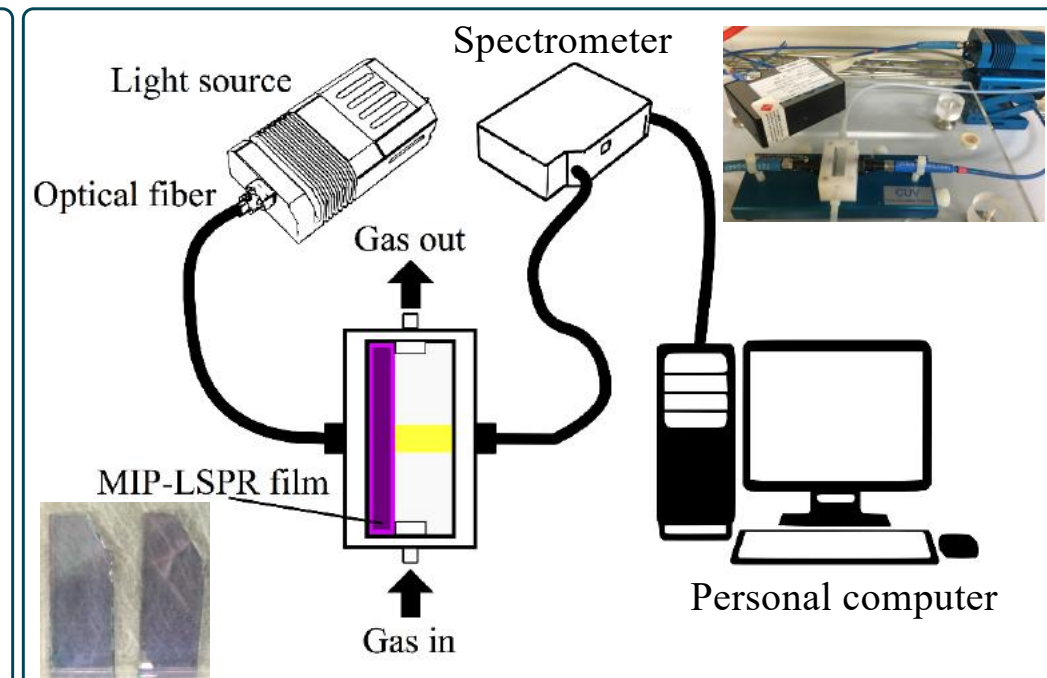
Experiment

Testing system



Gas generate system

$$k = \frac{22.4 \times (273 + t) \times 760}{M \times 273 \times P}$$



Transmittance spectra testing system

t – Thermodynamic temperature (°C)

M – Molecular weight (g/mol)

P – Atmosphere (mmHg)

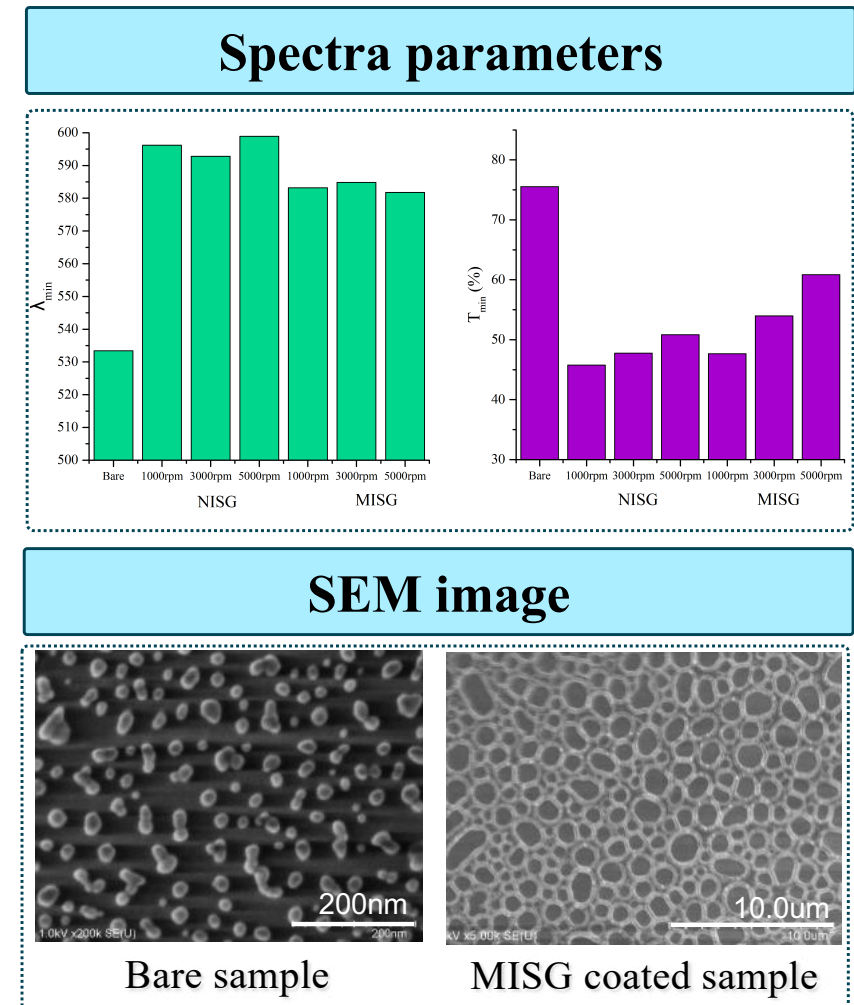
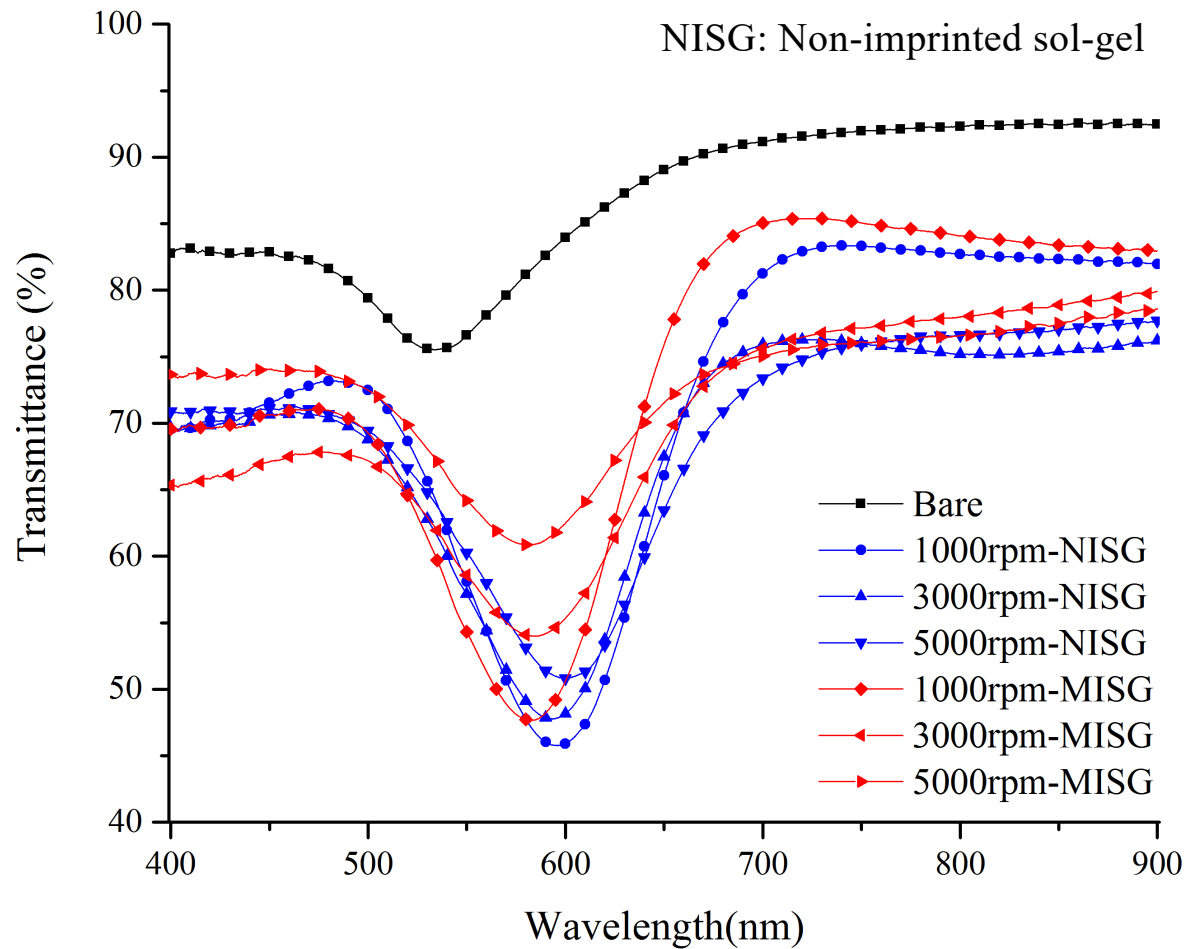
$$C = \frac{k \times D_r \times 10^3}{F}$$

Dr – Diffusion rate (μg/min)

F – Flow rate of dilute gas (ml/min)

Results and discussion

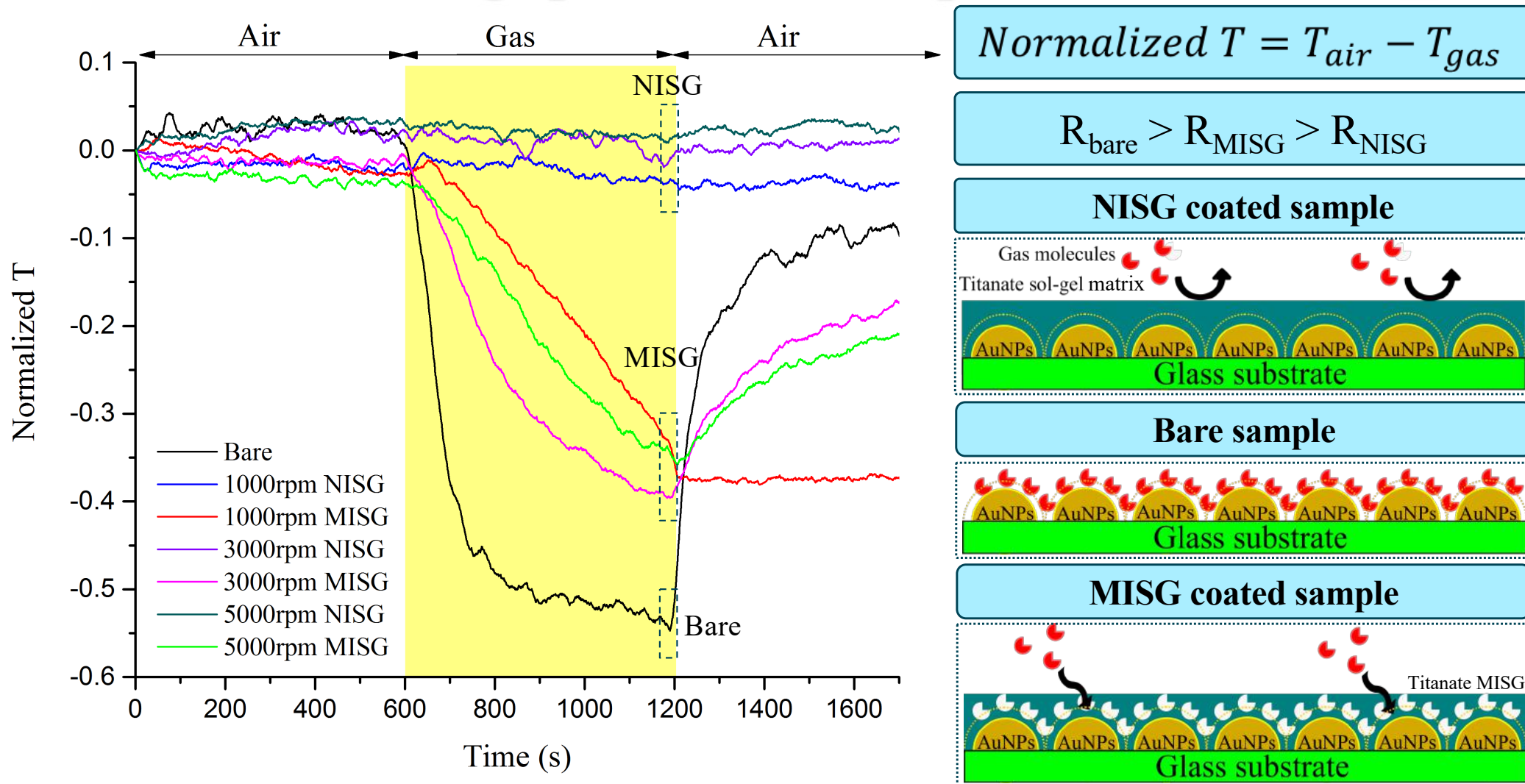
■ Transmittance spectra of MISG-LSPR sensors.



The changes of transmittance spectra are affected by their different surface features.

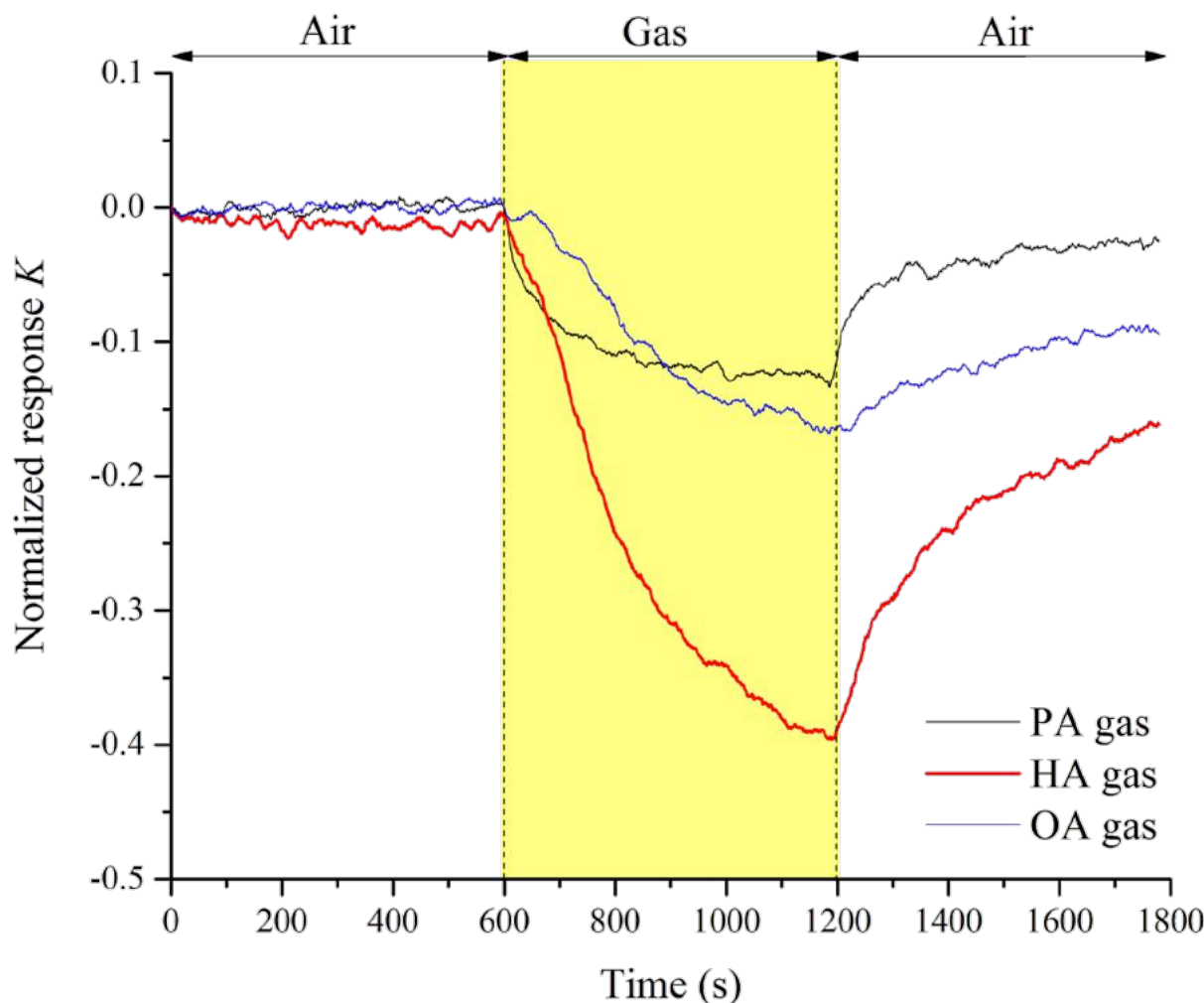
Results and discussion

■ Real-time response of HA-MISG and NISG with different coating speeds to HA vapors (Transmittance at λ_{\min})



Results and discussion

■ Real-time response of HA-MISG-LSPR sensor to three fatty acid vapors (PA/HA/OA)



HA-MISG-LSPR sensor

Template molecule: HA

Spin coating speed: 3000 rpm

PA: Propanoic acid (40.93 ppm)

HA: Hexanoic acid (21.05 ppm)

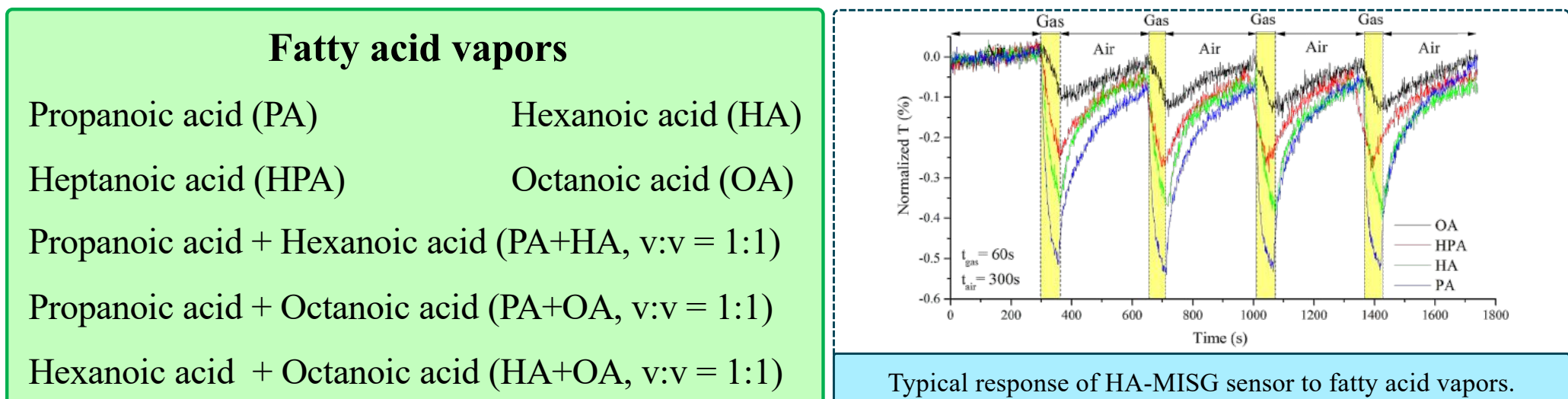
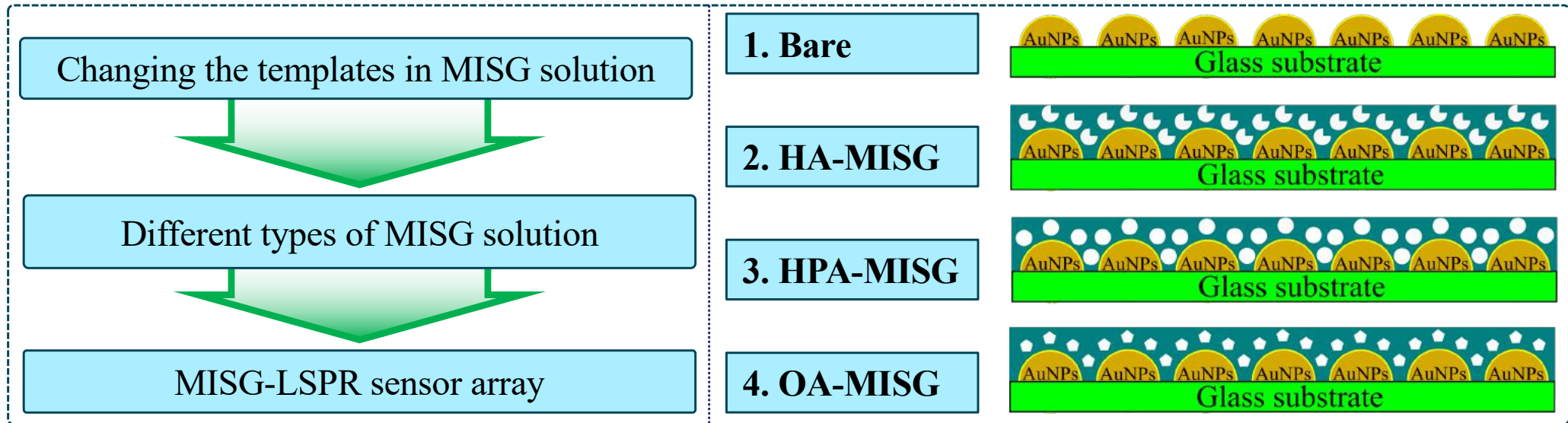
OA: Octanoic acid (11.23 ppm)

$$K = \text{Normalized } T/C_{\text{gas}}$$

A specific selectivity to HA vapors was obtained

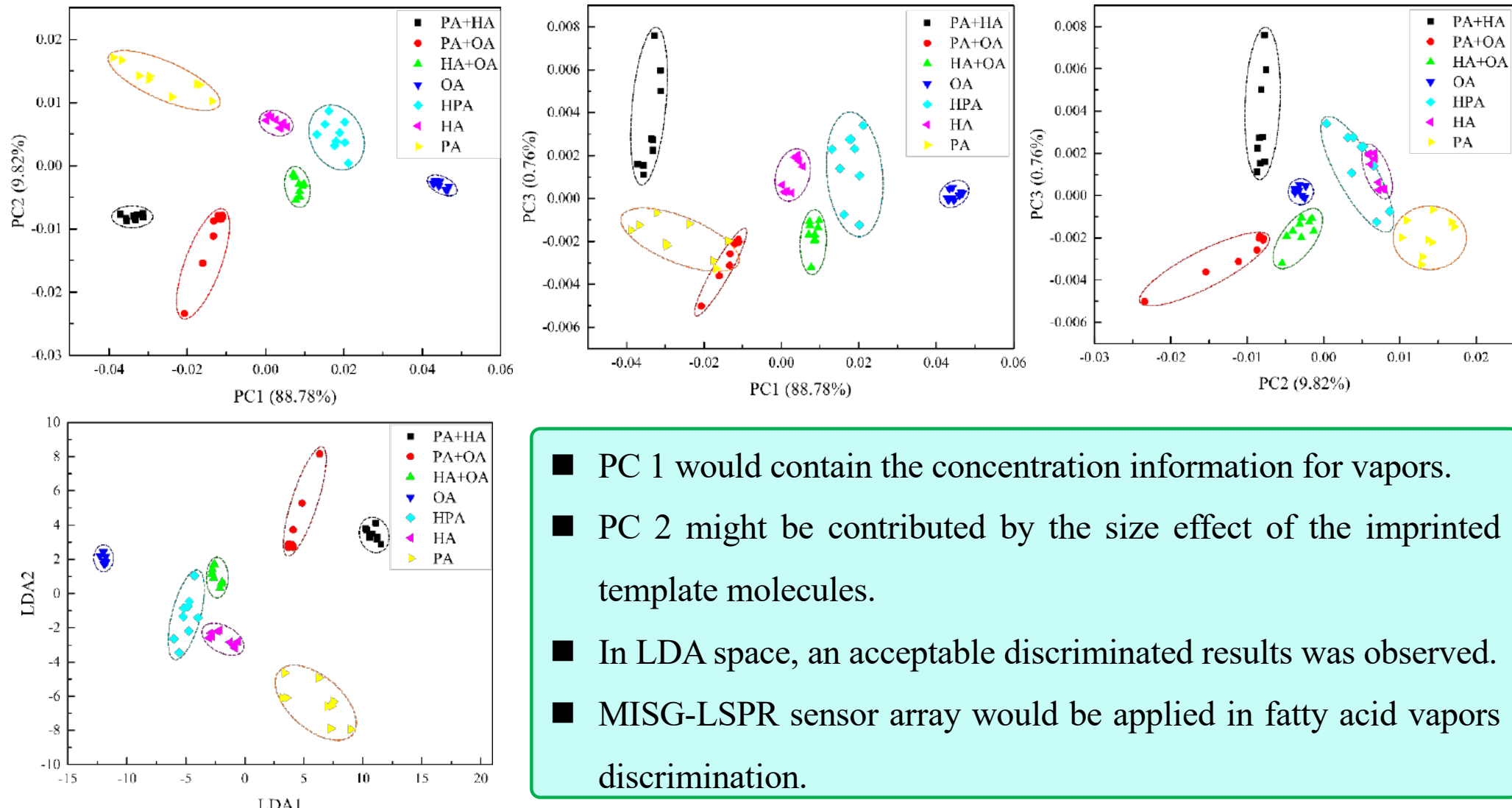
Results and discussion

■ MISG-LSPR sensor array for fatty acid vapors discrimination.



Results and discussion

■ PCA and linear discriminant analysis (LDA) results for diverse fatty acid vapors



Conclusion

- An AuNPs film combined with MISG was utilized for the determination of **fatty acid** vapors **selectively**.
- The **adsorption capacity** of pure titanate sol-gel matrix is **weak**.
- Molecules with similar structure to imprinted molecules (with carboxyl group, different carbon-chain length) were selected for MISGs selectivity evaluation.
- It indicated that **molecular information** can be obtained by MISGs.

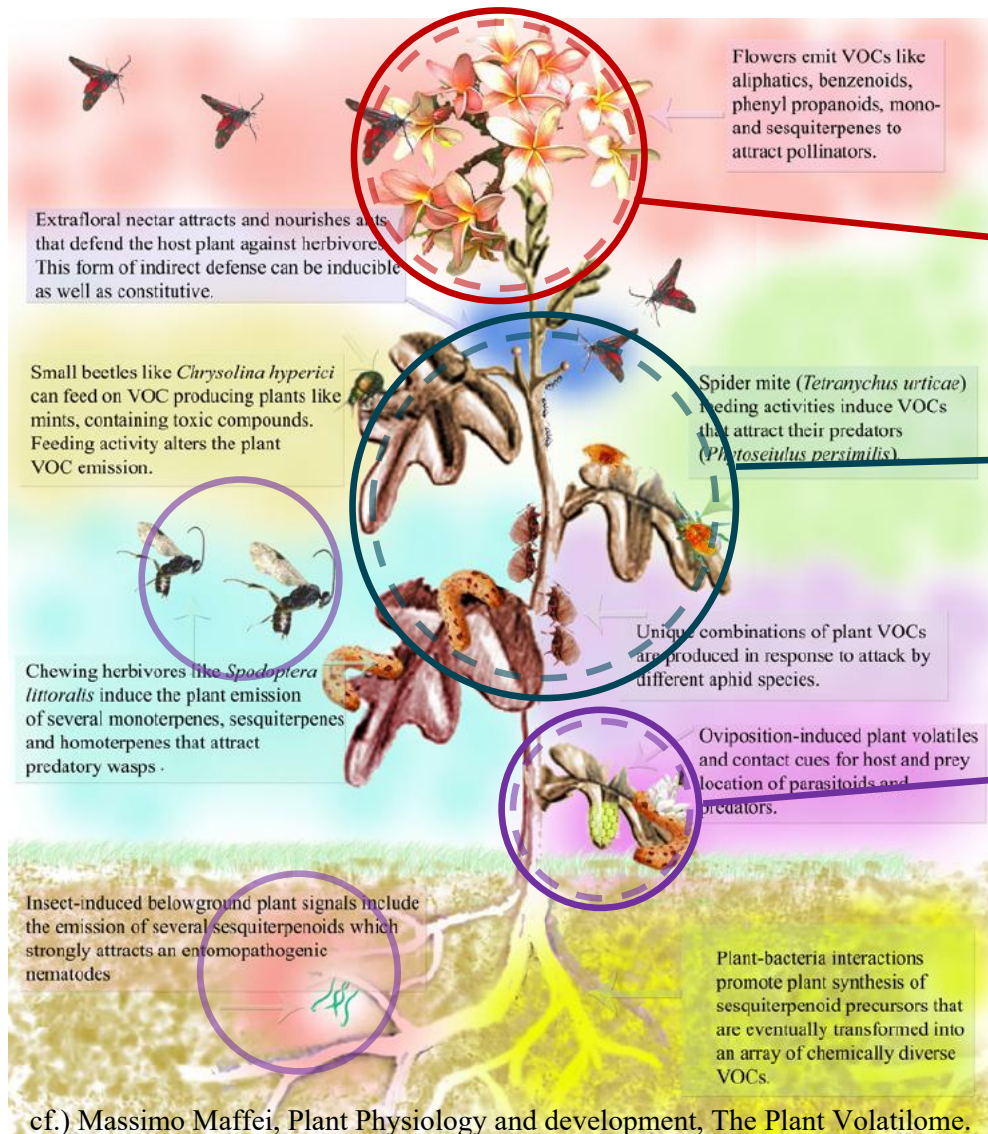
Chapter 5

Development of MISG based
LSPR sensor for detection of volatile
cis-jasmone



Introduction

Plant Volatile Organic Compounds (PVOCS)



Released from flowers, leaves, roots.

Attract pollinators

Plants self-protection

Spider mite

Small beetles

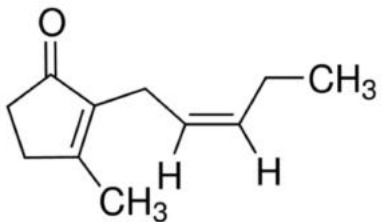
Act as wound sealers

Attract predators

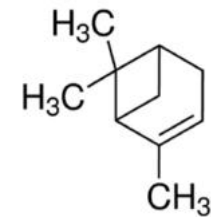
Plant–plant communication

Introduction

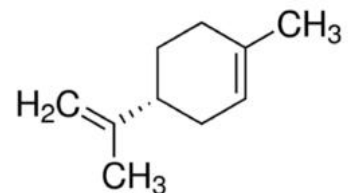
PVOCs



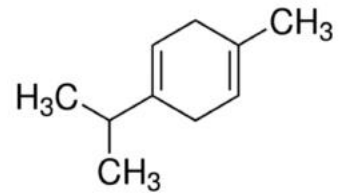
cis-Jasmone



α -Pinene



Limonene



γ -Terpinene



Application



Pest detection



Plant monitoring



Agriculture ICT

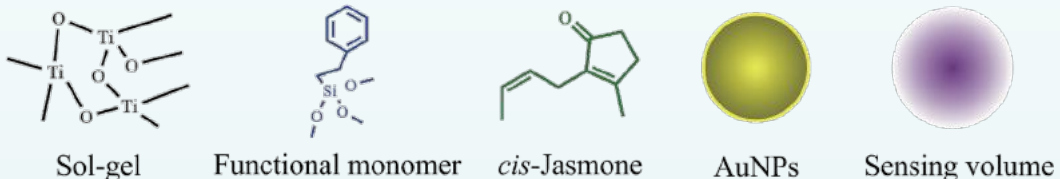
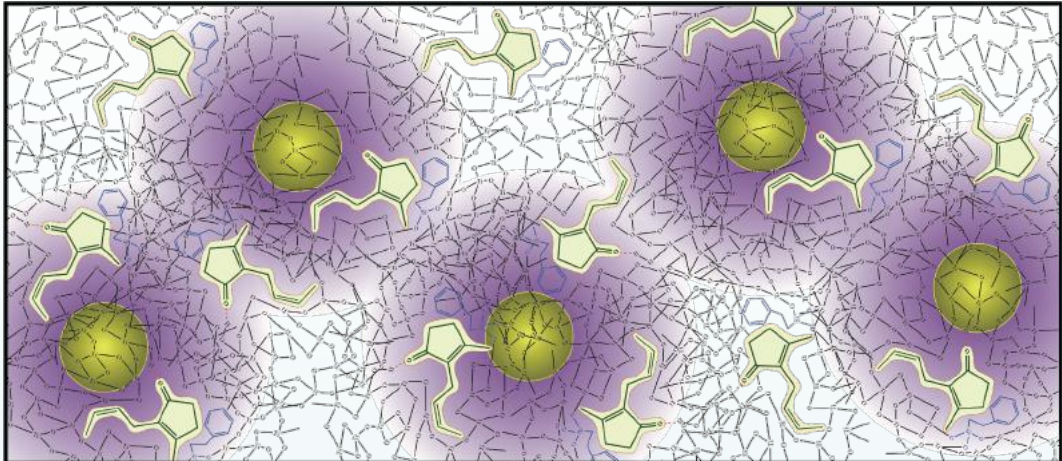
We need a translator for plants!

Gas chromatography/mass spectrometry
GC/MS

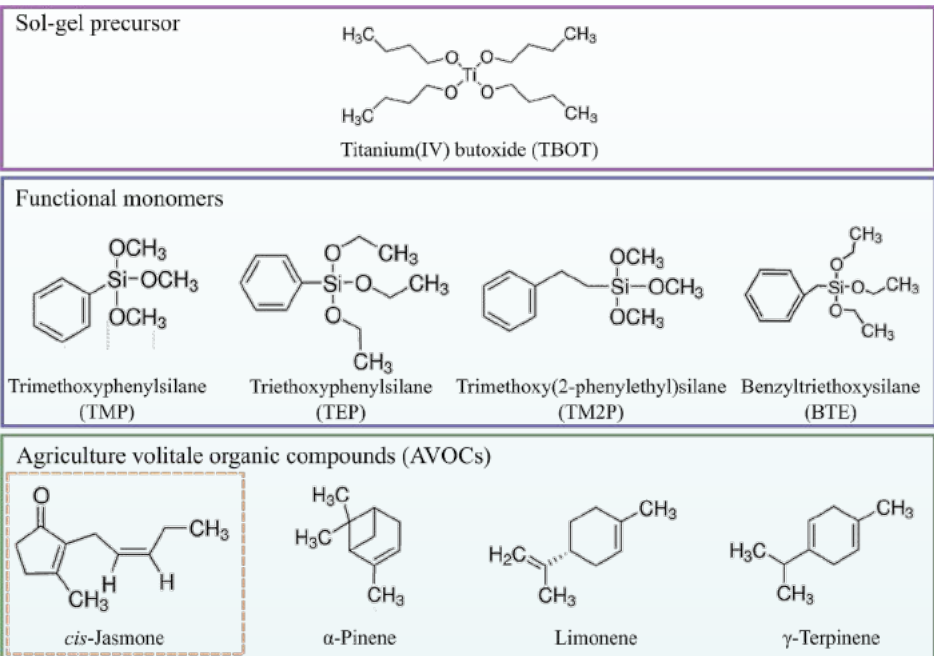
High-cost, not portable and
time-consuming

Not suitable for PVOCs real-time
monitoring

Concept



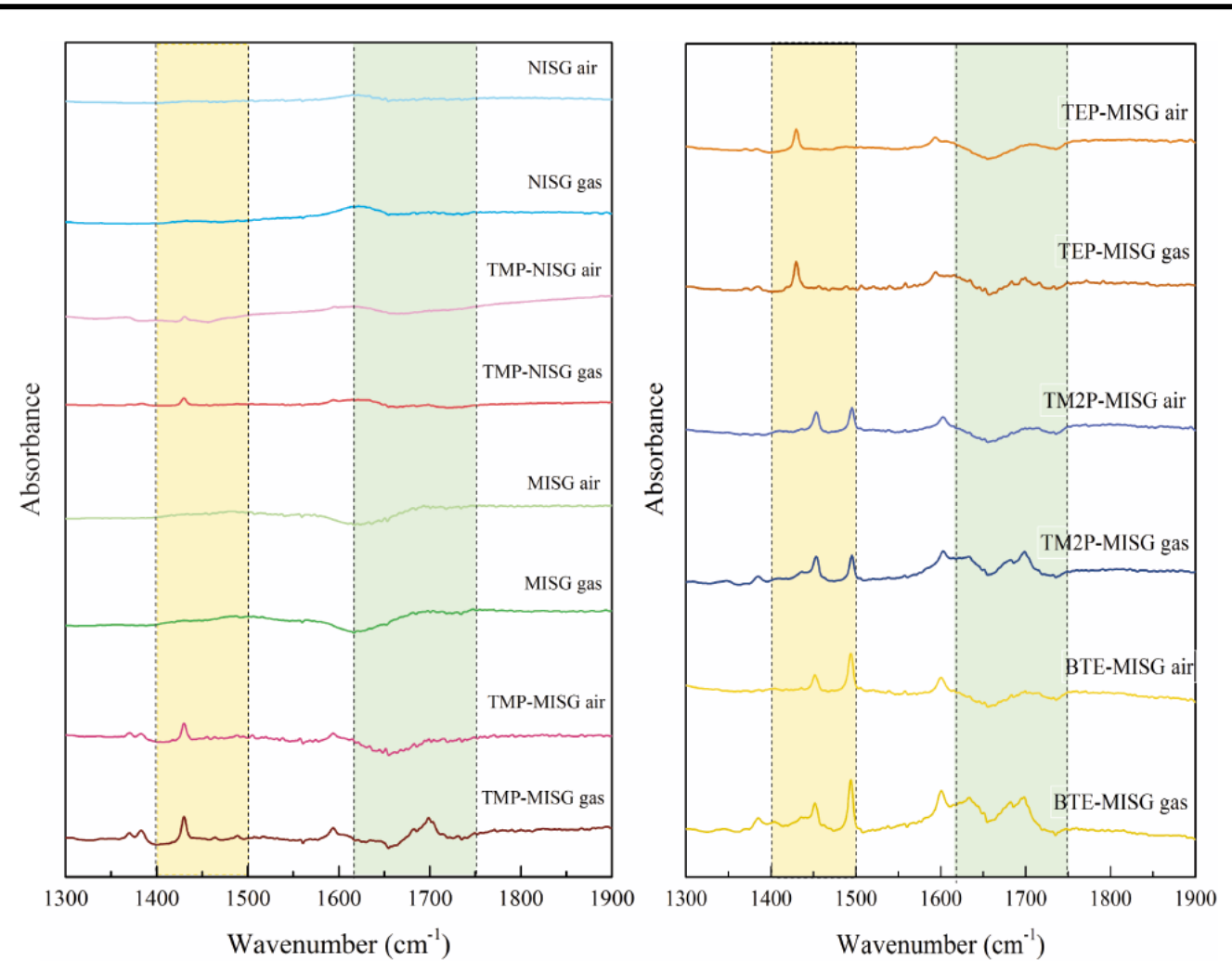
Schematic of MISG-coated Au nano-islands with functional monomers for selective CJ vapor detection.



Chemical structures of the matrix precursor, four functional monomers, and four types of PVOCS.

- The **functional monomer** was a critical for MISGs preparation.
- Functional monomers with **aromatic rings** would be appropriate for cavity generation in the MISGs via–electron, Van der Waals, and hydrogen-bond interactions.

Results and discussion



FT-IR spectra of NISG-, TMP-NISG-, MISG-, TMP-MISG-, TEP-MISG-, TM2P-MISG-, and BTE-MISG-coated samples before and after CJ vapor absorption.

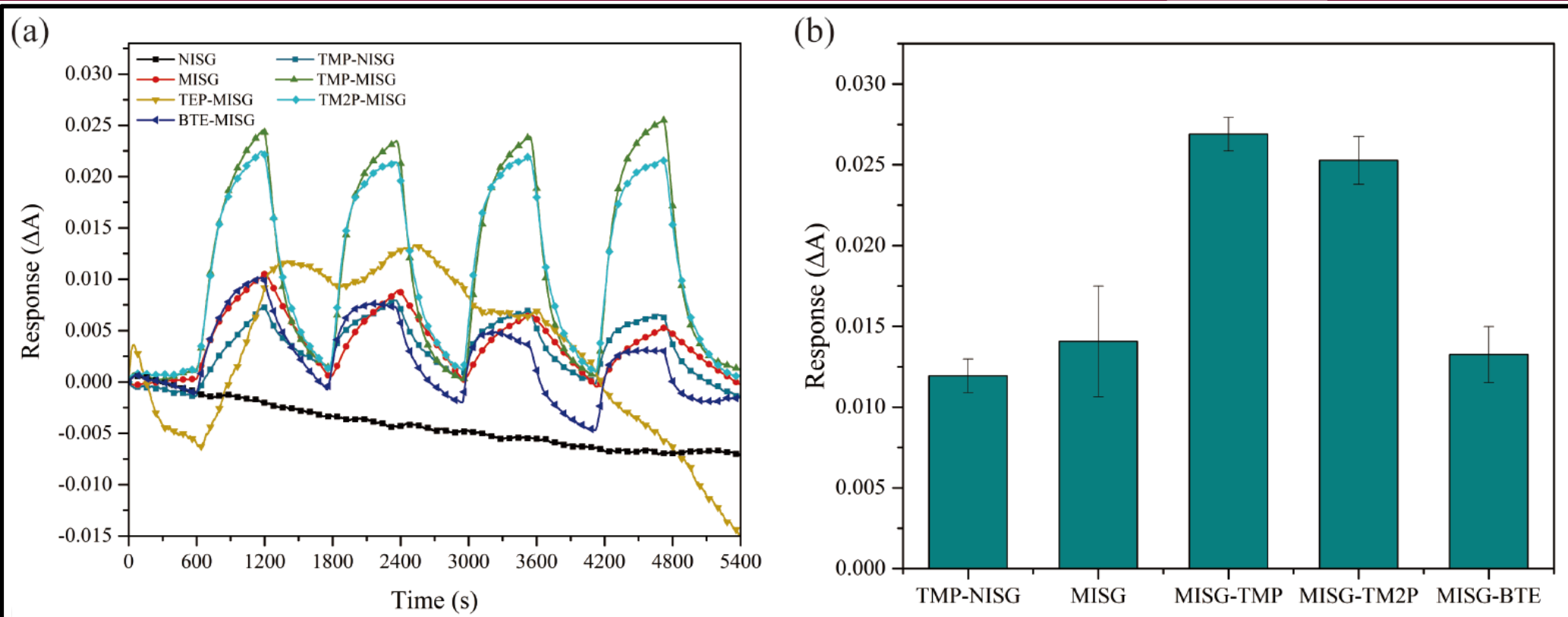
Benzoid ring peaks

- The monomers were polymerized in the sol-gel films.

C=O stretching

- Peak was observed in MISG-TMP- and MISG-TM2P-coated samples after gas absorption.
- Lower energy peaks appeared in the MISG- and MISG-BTE-coated samples.
- No peaks in the NISG-modified samples, which indicated less gas absorption.

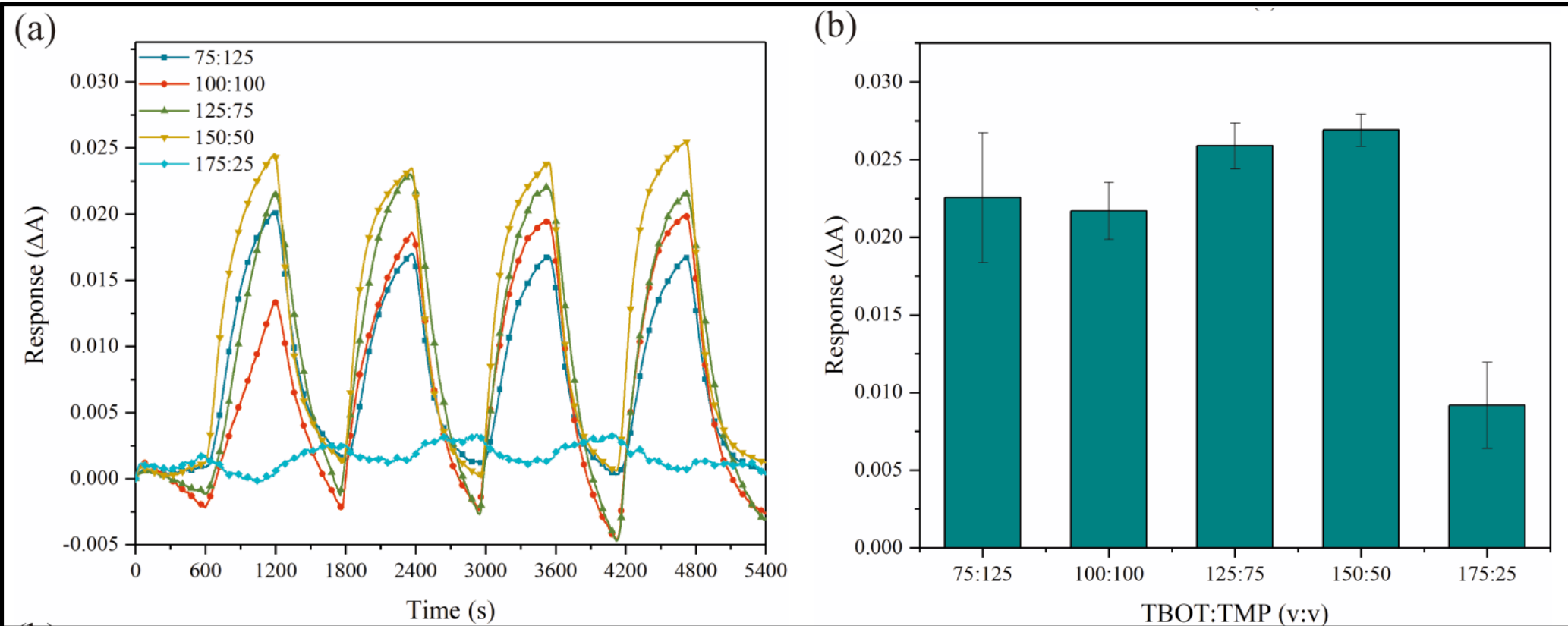
Results and discussion



Real-time responses for NISG-, MISG-, TMP-MISG-, TEP-MISG-, TM2P-MISG-, and BTE-MISG-coated samples (a) and their quantitative responses (b).

- No responses to CJ vapor were observed for NISG-modified sensors.
- MISGs without functional monomers exhibited lower.
- TMP appeared to be the optimal functional monomer.

Results and discussion

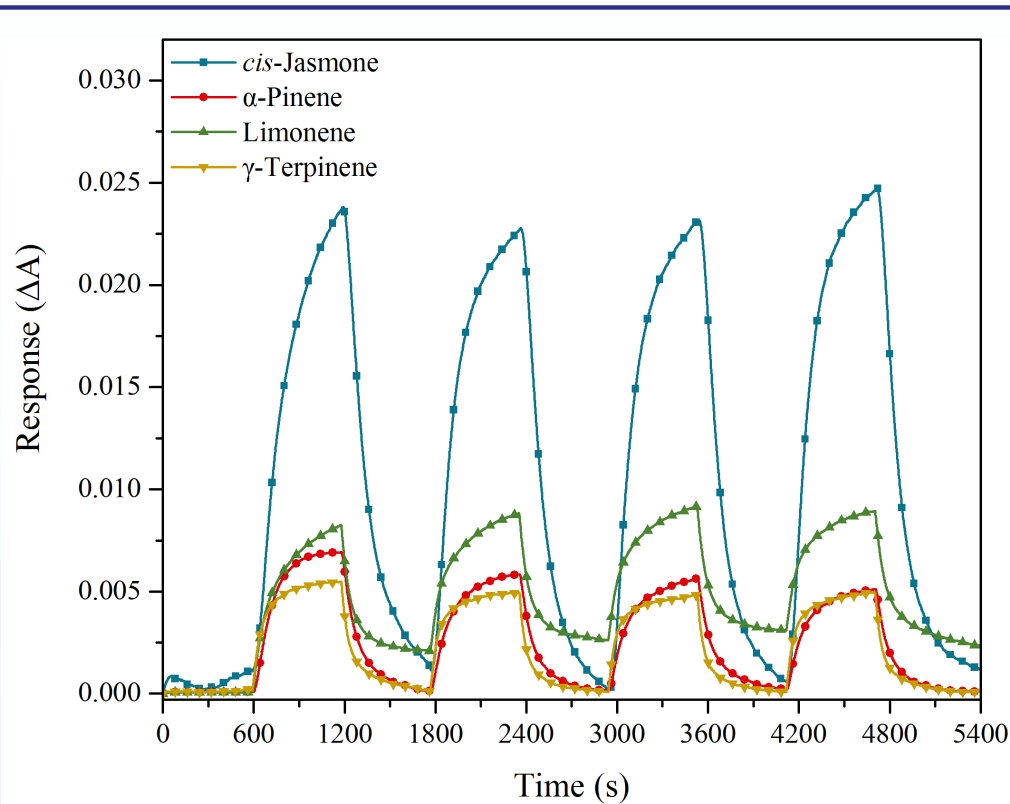


Real-time responses of samples coated with TMP-MISG at TBOT/TMP = 75/125, 100/100, 125/75, 150/50, 175/25 (v/v) (a) and their response summary (b).

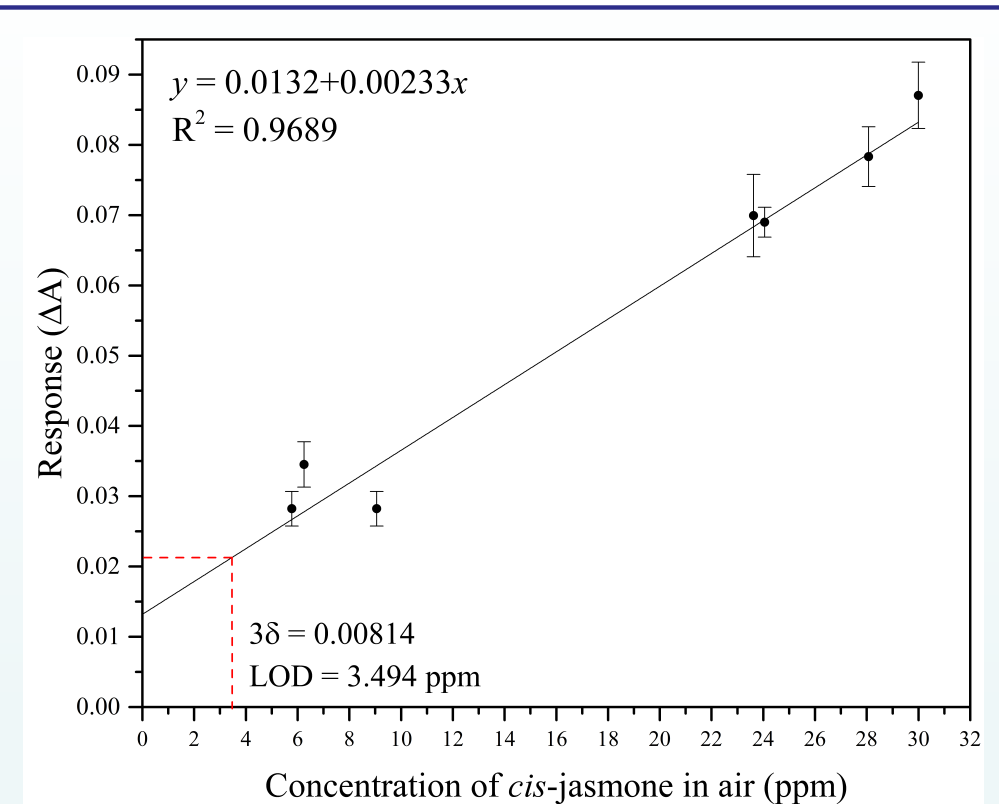
- Imprinting with MIP materials was affected by the ratio of the matrix/functional monomers.
- AuNPs coated by MISG-TMP with the ratio TBOT/TMP=150/50 had the highest CJ sensitivity.

Results and discussion

MISG-LSPR sensor



Real-time responses of TMP-MISG-LSPR sensor to 4 PVOCs.



The limit of detection (LOD) for *cis*-jasmone sensor was 3.494 ppm.

A specific selectivity to *cis*-jasmone vapors was obtained.

Conclusion

- LSPR sensors based on MISG-modified Au nano-islands was demonstrated for CJ vapor detection.
- Under optimal conditions, the volume ratio **TBOT/TMP = 150/50** resulted in a **3.494-ppm** LOD for CJ vapor.
- Real-time responses of the sensors displayed good selectivity, broad linearity, and repeatability.
- This study indicated that by adding FMs, the interaction between MISGs and molecules can be controlled, which can be applied for extracting functional group/polar information for VOCs.

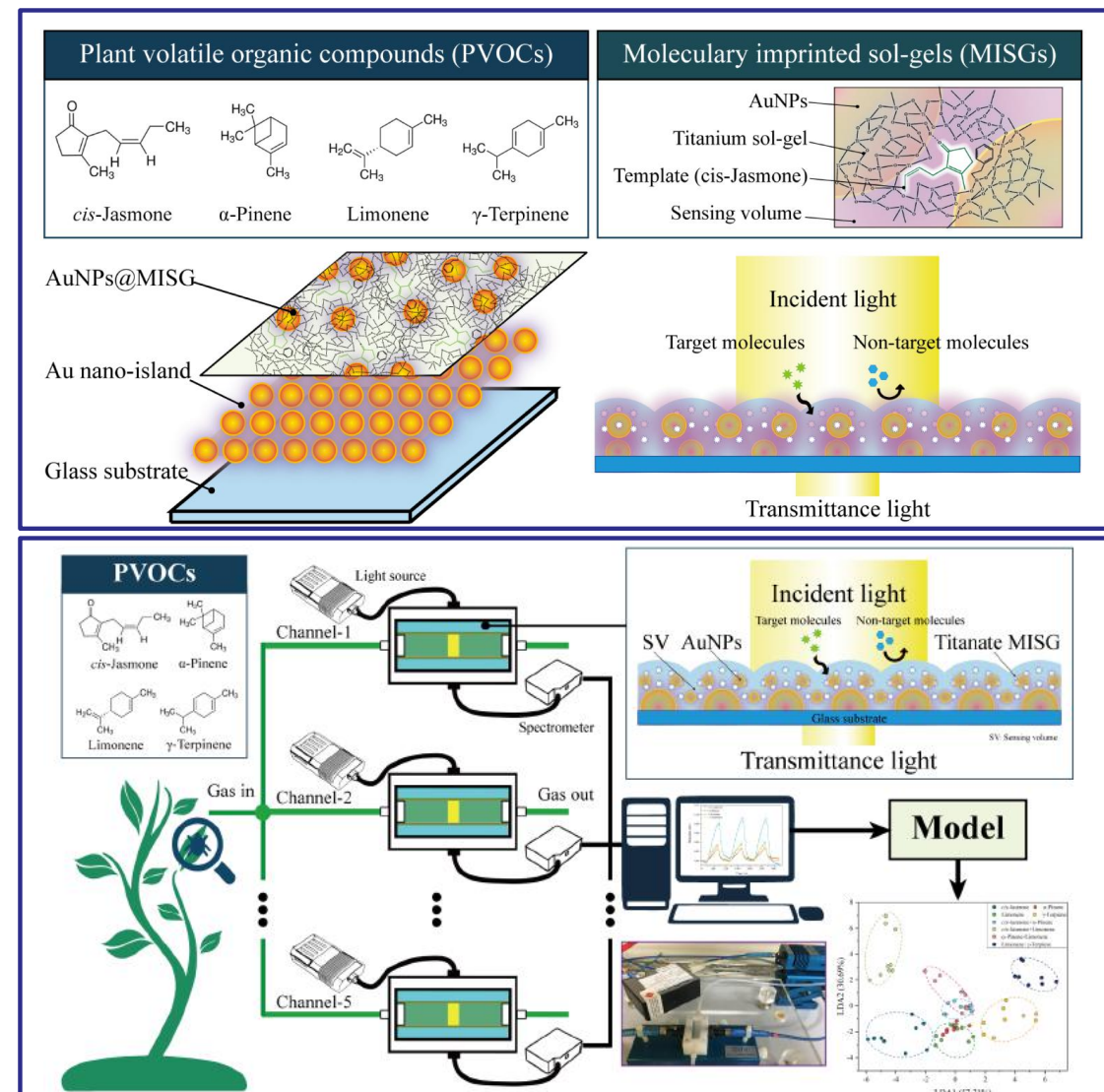
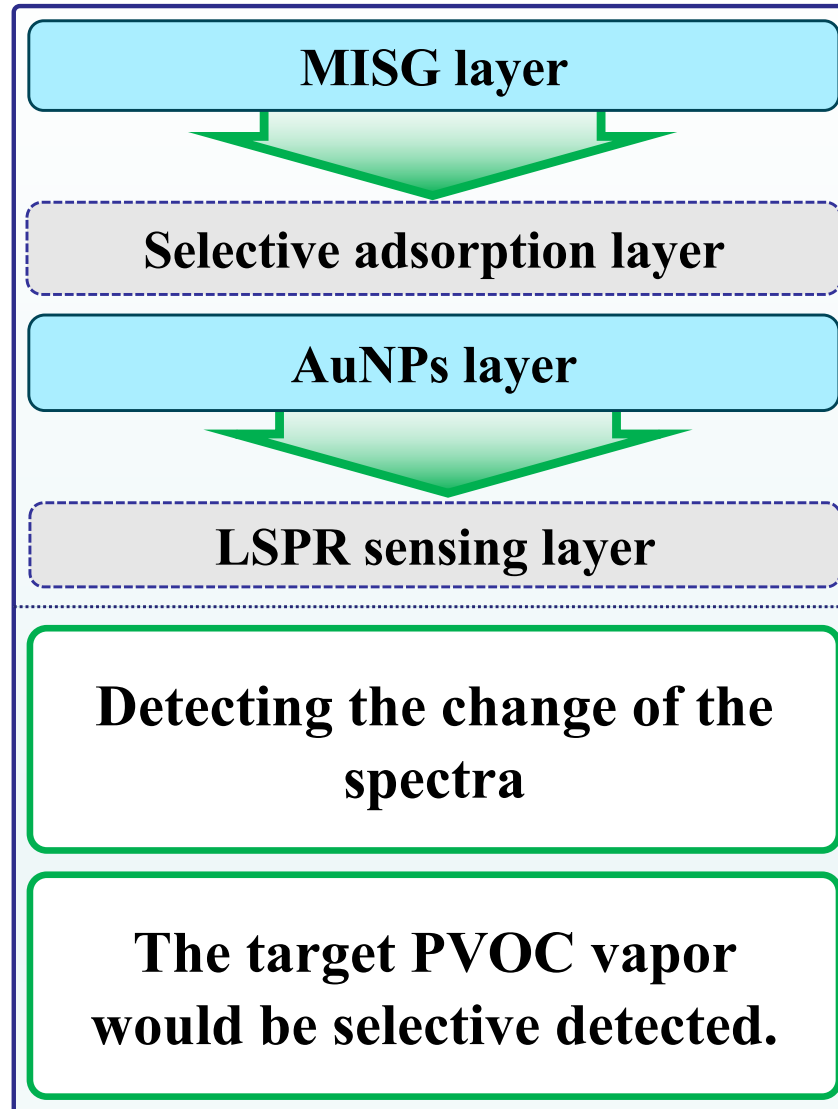
Chapter 6

LSPR Sensor Array Coated AuNPs@MISGs for PVOCs Recognition



Concept

MISG-LSPR sensor (AuNPs/MISG/AuNPs)



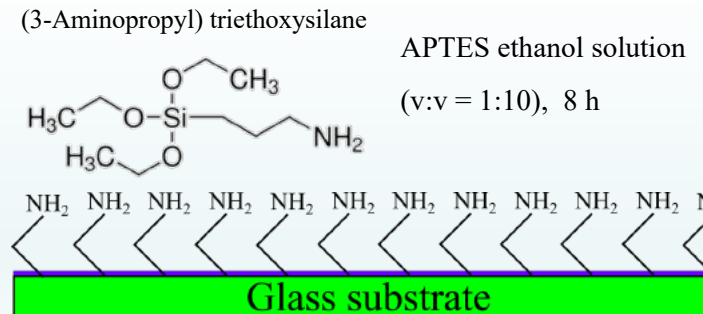
Experiment

MISG-AuNPs

Iso-propanol	2 mL
Ti(OBu) ₄	150 μ L
TMP	25 μ L
Template	50 μ L
TiCl ₄	25 μ L

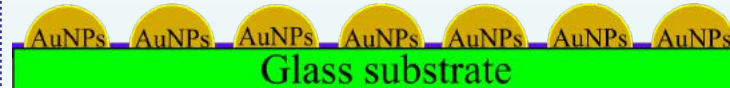
MISG-AuNPs film fabrication

Step 1 APTES modification



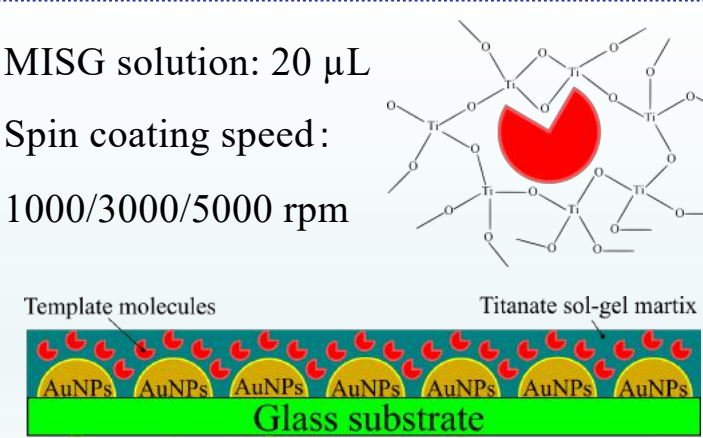
Step 2 Sputtered AuNPs and anneal

Sputtering AuNPs thickness: 3nm
Anneal: 500 °C, 2 h, 2 times, air



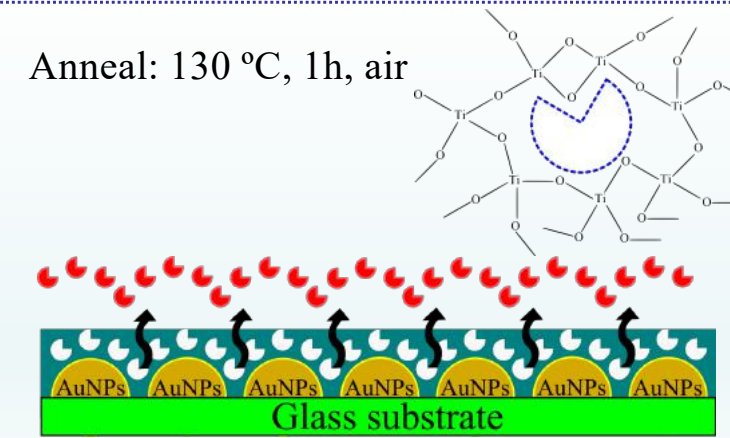
Step 3 MISG reaction solution spin coating

MISG solution: 20 μ L
Spin coating speed:
1000/3000/5000 rpm



Step 4 Annealed for removing templates

Anneal: 130 °C, 1h, air

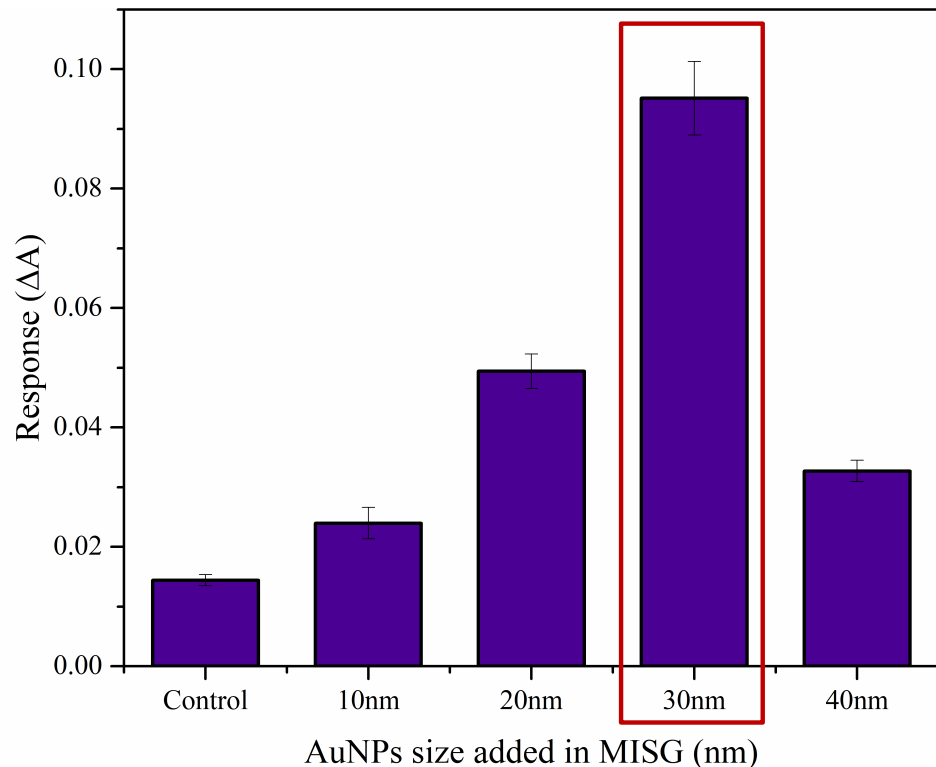


60 °C water bath, 1h

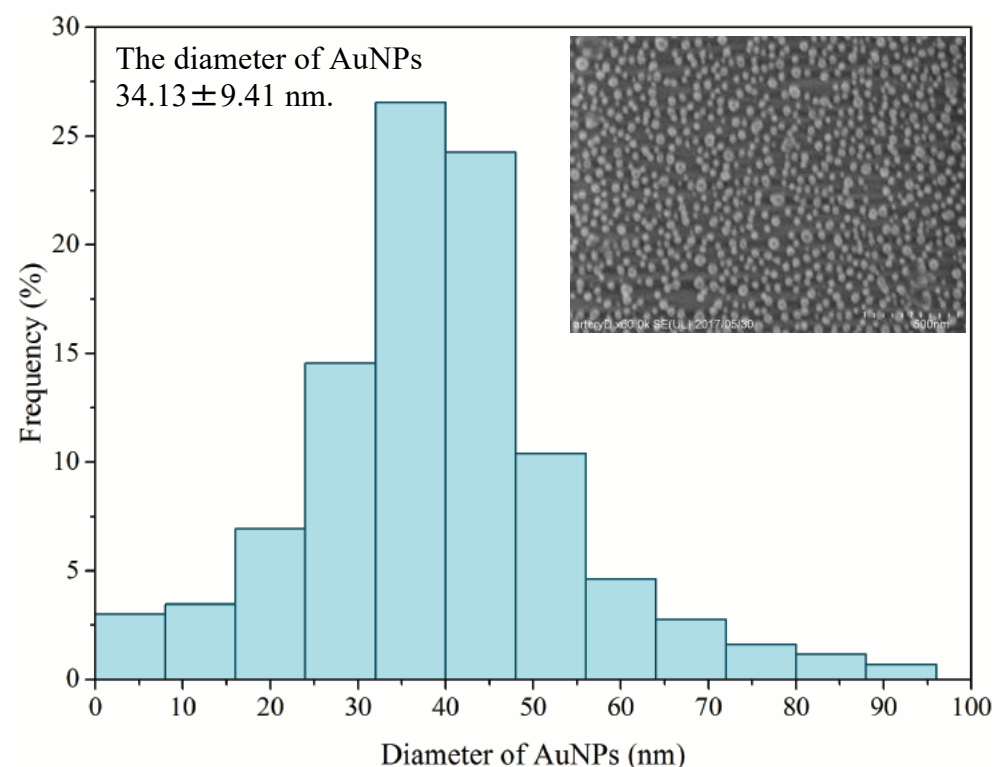
AuNPs solution

Stirring 4h

Results and discussion



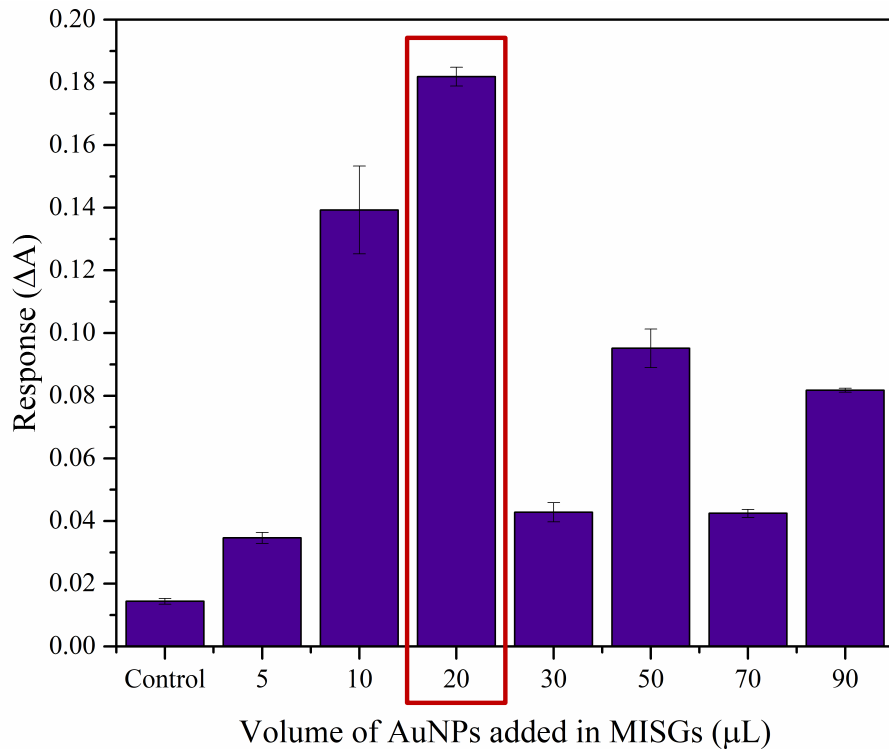
Response effected by AuNPs size in MISGs.



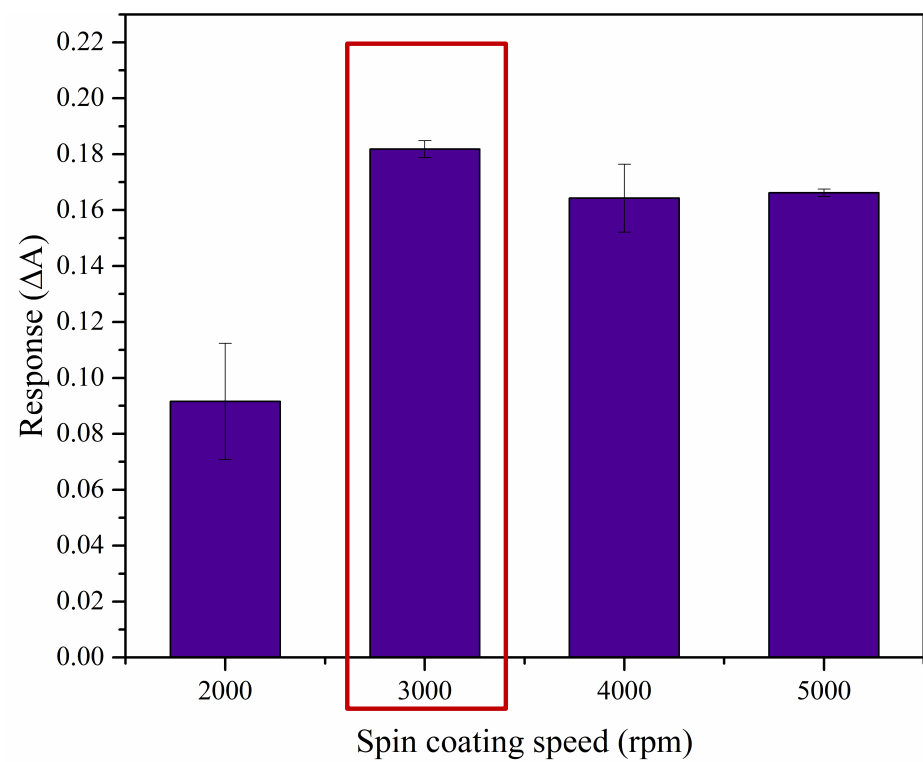
Particle size distribution histogram of spherical AuNPs determined from bare sample.

- Response of AuNPs@MISG-coated with 30-nm AuNPs was 6.33 times that of the one without NPs.
- The diameter of the AuNPs on the substrate is close to that of the AuNPs in the MISG (30 nm).
- The high sensitivity of the sensor was contributed by hot-spot coupling.

Results and discussion



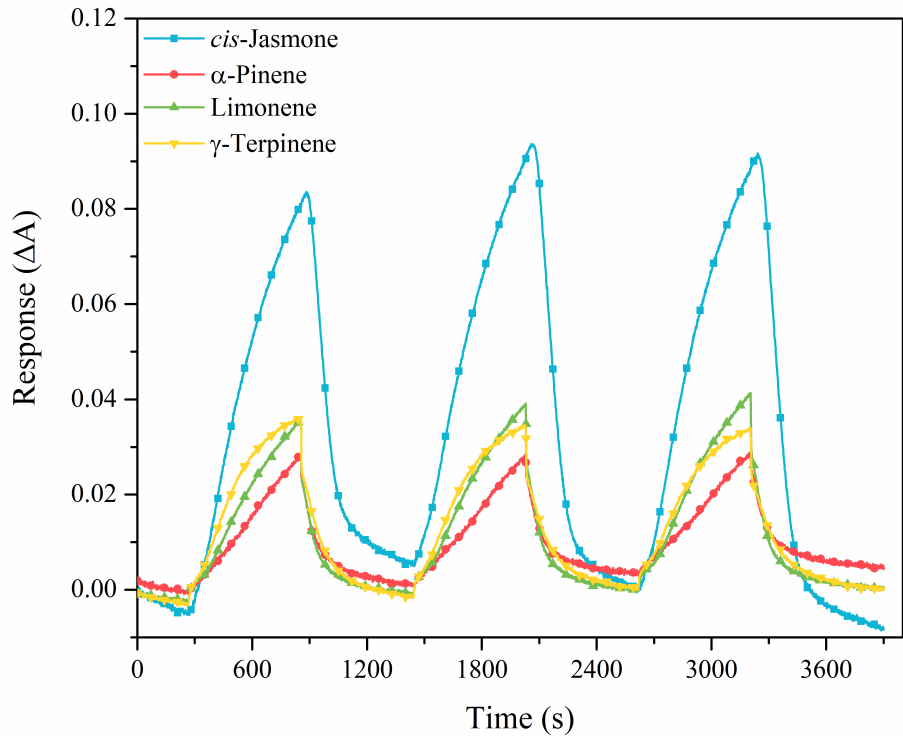
Response effected by AuNPs (30 nm) amount in MISGs.



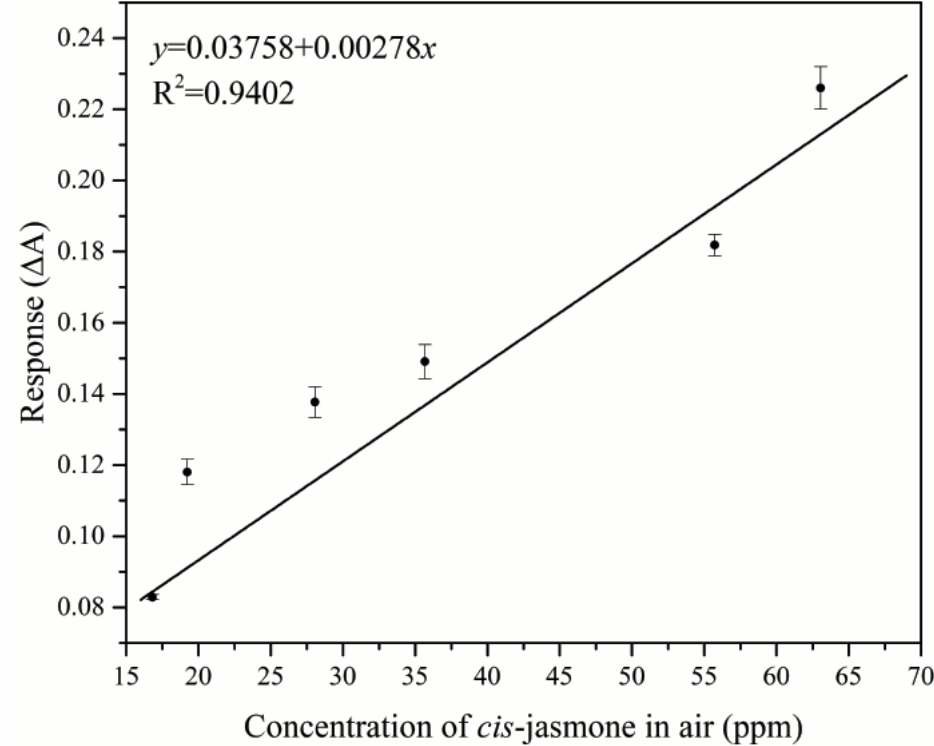
Response effected by spin coating speed.

- Sensitivity of the sensors increased with the AuNP concentration initially and then decreased.
- Sensor coated with the MISG containing 20 μL AuNPs had the highest sensitivity.
- The thickness of the sensing film influences the sensitivity of LSPR sensors.
- Optimal spin coating speed was selected as 3000 rpm in the present study.

Results and discussion



Real-time responses of AuNPs@MISG-modified Au-islands to 4 PVOCs.



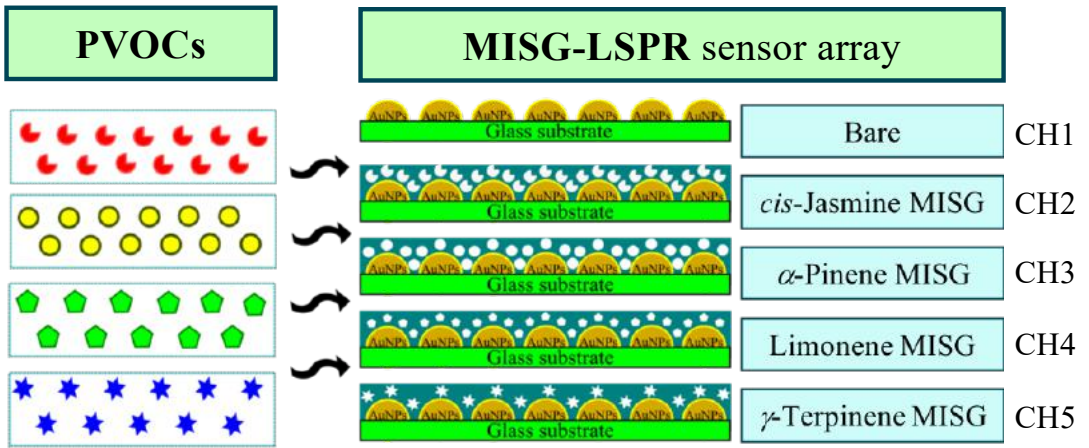
Linear response vs. CJ concentration in air.

- Response to CJ was much higher than that to the interfering plant VOCs (Interference immunity).
- The limited of detection (LOD) was calculated as 3.07 ppm (S/N=3).
- The developed sensor has sufficient interference immunity for use in agricultural applications.

Results and discussion

Sensor response matrix to PVOCS

MISG-LSPR sensor array



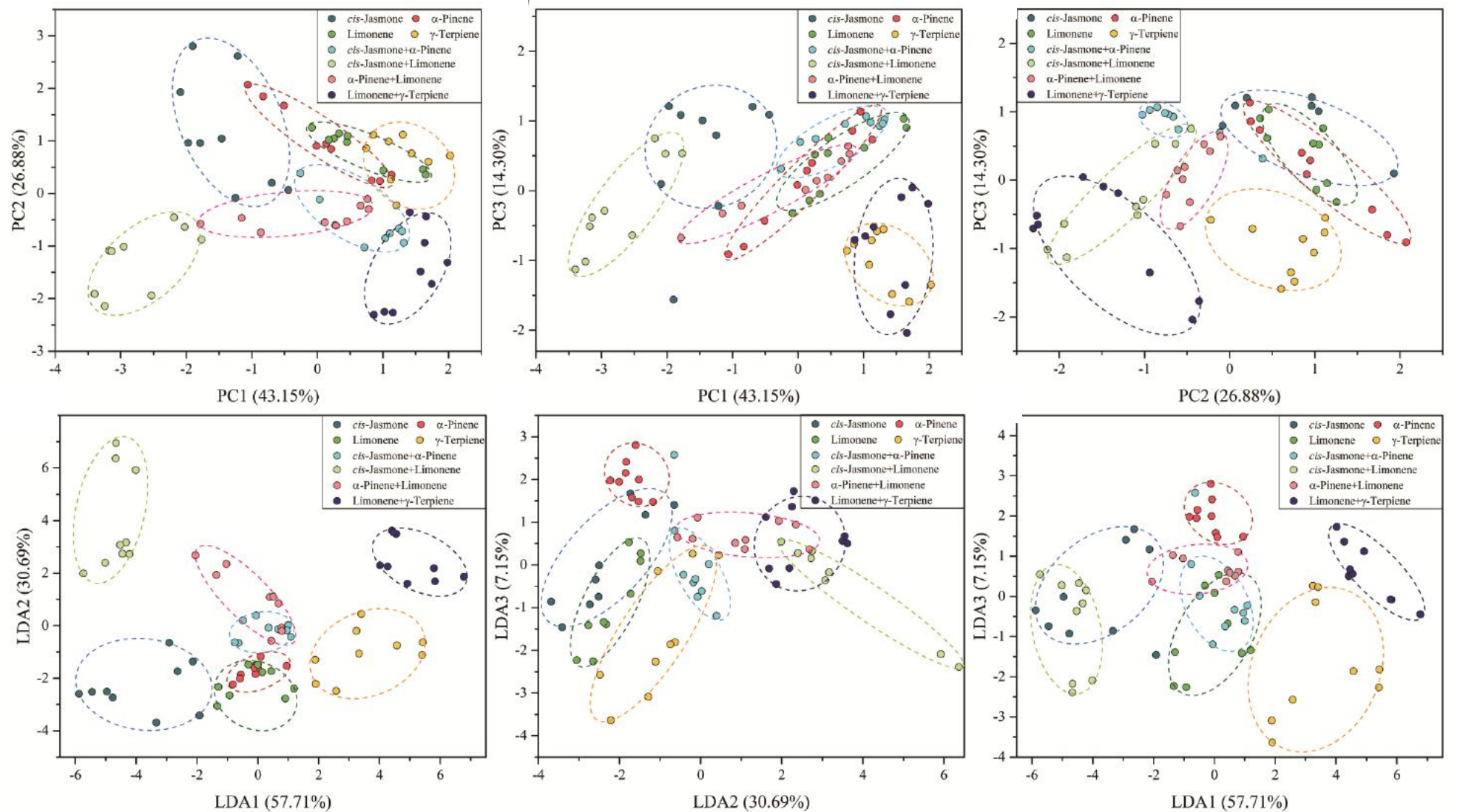
- By changing the flow rates (0.3, 0.5 and 0.7 L/min), PVOCS with different concentrations would be obtained.
- 72 samples (8 PVOCS × 3 flow rates × 3 repeats) were obtained in this study.
- All responses were scaled for former processing.

Correlation matrix for channels

	CH1	CH2	CH3	CH4	CH5
CH1	1	0.06	-0.05	-0.17	-0.34
CH2	0.06	1	0.53	0.31	0.06
CH3	-0.05	0.53	1	0.59	0.1
CH4	-0.17	0.31	0.59	1	0.51
CH5	-0.34	0.06	0.1	0.51	1

- Low correlation between each channels.
- More information can be obtained in MISG sensor array.

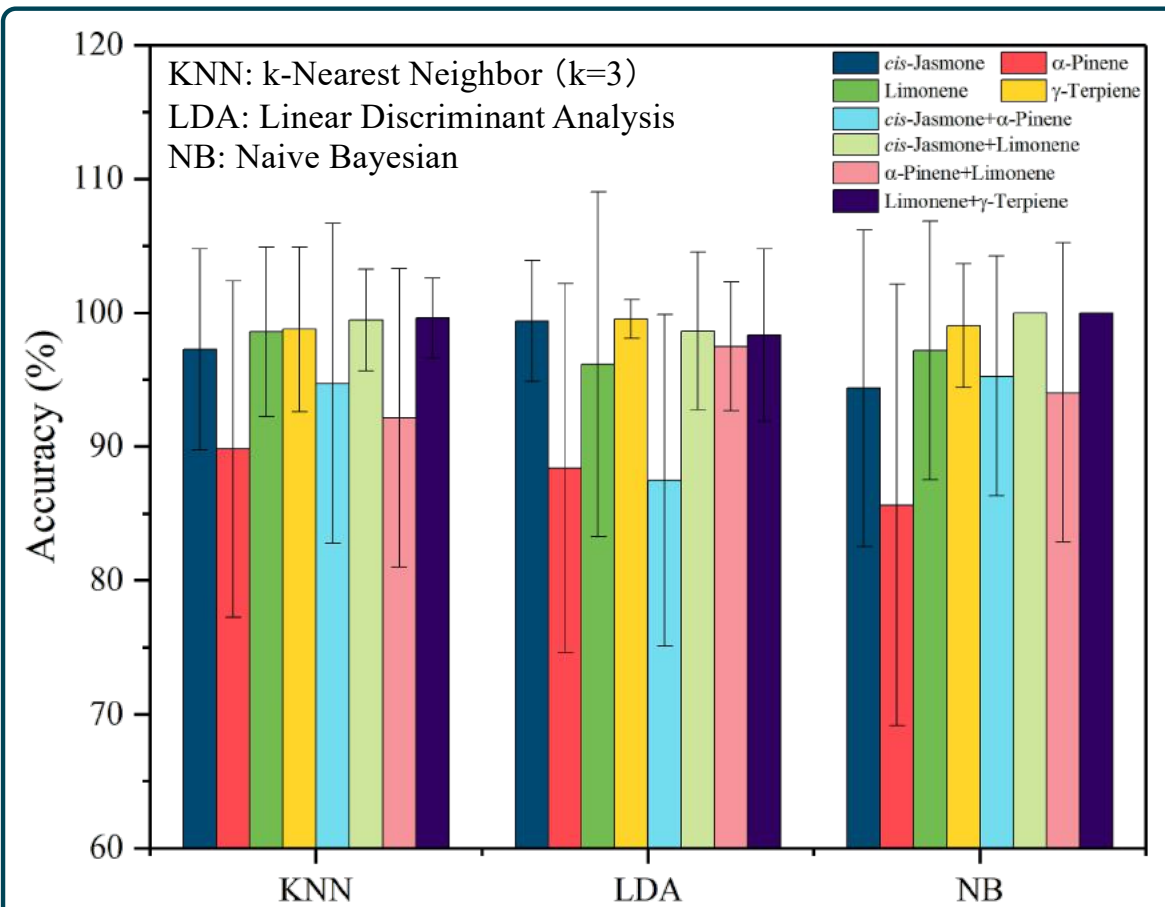
Results and discussion



Mapping samples in PCA space and LDA space

Results and discussion

Models established by KNN, LDA, and NB.



- Data sets were divided by random selection method.
- Train set : test set = 7:3. Repeat 100 times.

Models evaluation

Model	Accuracy	SD.
KNN	96.76 %	9.36 %
LDA	95.67 %	11.06 %
NB	95.72 %	11.48 %

Discussion

- PVOCS from single or mixture can be recognized and classified.
- Low accuracy in detecting α -pinene.
- In summary, KNN shown the best result than other models.
- Better result would be obtained by more samples.

Conclusion

- An LSPR sensor coated with an MISG containing AuNPs to amplify the sensing signal was developed for plant VOC detection.
- The sensitivity of the AuNPs@MISG-coated sensor was 12.33 times higher than that of the sample without AuNPs.
- The real-time responses of the sensor displayed good interference immunity and repeatability.
- A five-channel AuNPs@MISG LSPR sensor array was designed to detect and identify four plant VOCs alone and in binary mixtures.
- A large sensor array coated different MISGs would be developed for molecular information extraction.

Chapter 7

Conclusion



九州大学
KYUSHU UNIVERSITY

Conclusion

Structure–odor relationship

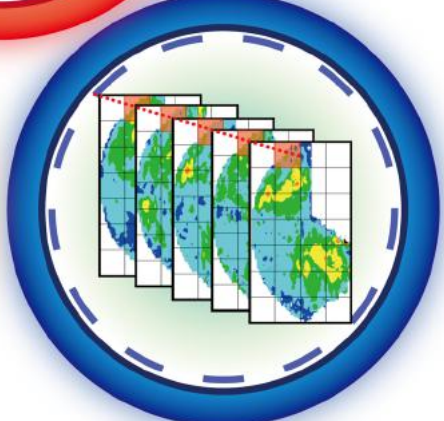
- Chapter 2 explored the correlation between odor maps and the molecular parameters.
- A comparative model could be established if it was based on enough molecular features.

- Chapter 3 present a model by which odor information can be obtained by machine-learning-based prediction from MPs of odorant molecules.
- Molecular parameters associated with machine-learning models can be adopted for odor perceptual senses identification.

Odor descriptions



Molecular parameters

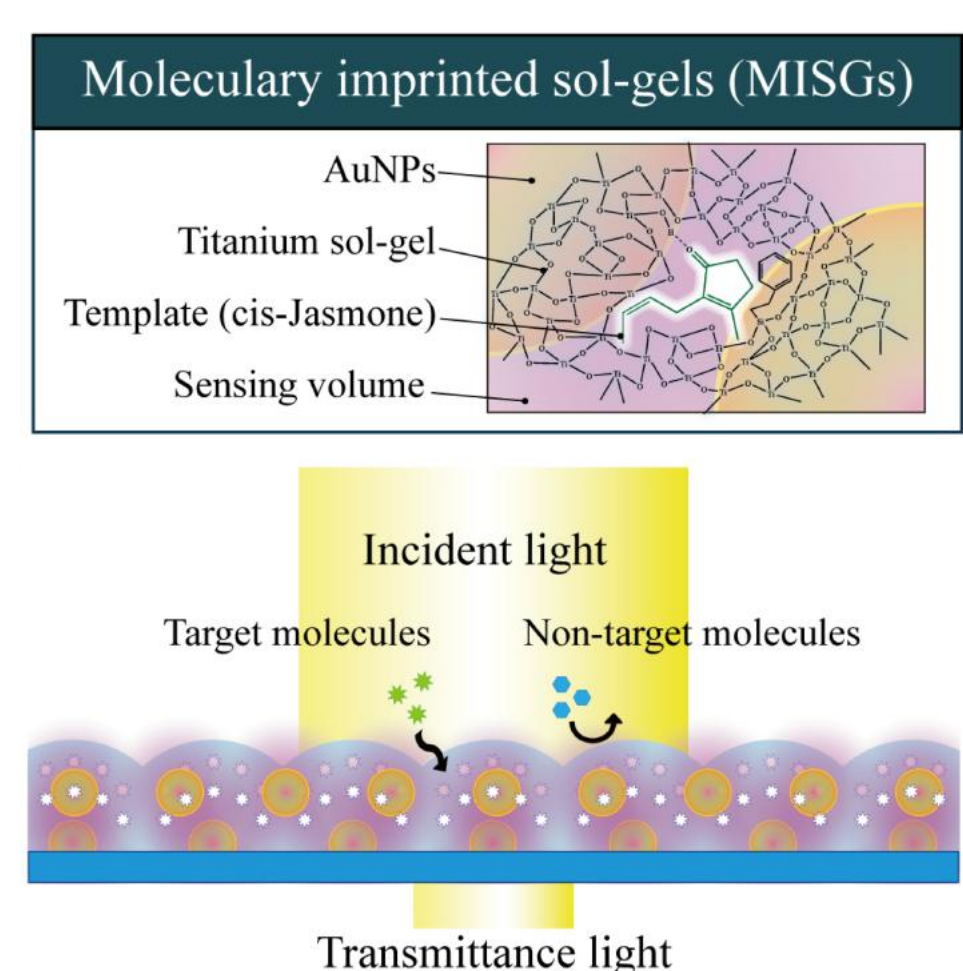


Odor maps

Conclusion

Molecular imprinted material coated optical odor sensor

- Chapter 4-6 explored the MISGs-LSPR sensor for determination of organic vapors selectively.
- The selectivity of MISGs can be controlled by functional monomers and template molecules.
- Furthermore, AuNPs were doped in MISGs for enhancing response intensity by hot spots generation.
- A multi-channel sensor platform was developed to detect VOCs in single and binary mixtures.
- The molecular parameters such as carbon chain length, size, polar and functional group can be detected.



Thank you for your attention

